REPORT NO. NADC-78259-60

CERTIFICATION OF COMPOSITE AIRCRAFT STRUCTURES
UNDER IMPACT, FATIGUE AND ENVIRONMENTAL CONDITIONS

PART II

SCALE EFFECT IN FATIGUE OF COMPOSITE MATERIALS

Pei Chi Chou and Robert Cronmen
DREXEL UNIVERSITY
Philadelphia, Pennsylvania 19104

JANUARY 1978

DTIC QUALITY INSPECTED 3

Prepared for
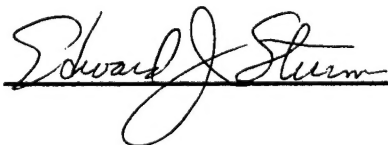NAVAL AIR DEVELOPMENT CENTER
Warminster, Pennsylvania 18974

NOTICES

REPORT NUMBERING SYSTEM - The numbering of technical project reports issued by the Naval Air Development Center is arranged for specific identification purposes. Each number consists of the Center acronym, the calendar year in which the number was assigned, the sequence number of the report within the specific calendar year, and the official 2-digit correspondence code of the Command Office or the Functional Directorate responsible for the report. For example: Report No. NADC-78015-20 indicates the fifteeth Center report for the year 1978, and prepared by the Systems Directorate. The numerical codes are as follows:

CODE	OFFICE OR DIRECTORATE
00	Commander, Naval Air Development Center
01	Technical Director, Naval Air Development Center
02	Comptroller
10	Directorate Command Projects
20	Systems Directorate
30	Sensors & Avionics Technology Directorate
40	Communication & Navigation Technology Directorate
50	Software Computer Directorate
60	Aircraft & Crew Systems Technology Directorate
70	Planning Assessment Resources
80	Engineering Support Group

PRODUCT ENDORSEMENT - The discussion or instructions concerning commercial products herein do not constitute an endorsement by the Government nor do they convey or imply the license or right to use such products.

APPROVED BY: _Edward J Sturm_____ DATE: _17 November 1978_

UNCLASSIFIED

REPORT NO. NADC-78259-60

CERTIFICATION OF COMPOSITE AIRCRAFT STRUCTURES
UNDER IMPACT, FATIGUE AND ENVIRONMENTAL CONDITIONS

PART II

SCALE EFFECT IN FATIGUE OF COMPOSITE MATERIALS

Pei Chi Chou
Robert Croman
DREXEL UNIVERSITY
Philadelphia, Pennsylvania

January 1978

UNCLASSIFIED

SECURITY CLASSIFICATION OF THIS PAGE *(When Data Entered)*

REPORT DOCUMENTATION PAGE	READ INSTRUCTIONS BEFORE COMPLETING FORM

1. REPORT NUMBER NADC-78259-60	2. GOVT ACCESSION NO.	3. RECIPIENT'S CATALOG NUMBER

4. TITLE *(and Subtitle)* Certification of Composite Aircraft Structures under Impact, Fatigue and Environmental Conditions. Part II-Scale Effect in Fatigue of Composite Materials	5. TYPE OF REPORT & PERIOD COVERED Final Contract Report July 1 1976 – Dec. 31 1977
	6. PERFORMING ORG. REPORT NUMBER

7. AUTHOR(s) Pei Chi Chou and Robert Croman	8. CONTRACT OR GRANT NUMBER(s) N62269-76-C-0378

9. PERFORMING ORGANIZATION NAME AND ADDRESS Drexel University Philadelphia, PA 19104	10. PROGRAM ELEMENT, PROJECT, TASK AREA & WORK UNIT NUMBERS

11. CONTROLLING OFFICE NAME AND ADDRESS Aircraft and Crew Systems Technology Directorate Naval Air Development Center Warminster, PA 18974	12. REPORT DATE
	13. NUMBER OF PAGES 64

14. MONITORING AGENCY NAME & ADDRESS*(if different from Controlling Office)*	15. SECURITY CLASS. *(of this report)* Unclassified
	15a. DECLASSIFICATION/DOWNGRADING SCHEDULE

16. DISTRIBUTION STATEMENT *(of this Report)*

Approved for Public Release; distribution unlimited.

17. DISTRIBUTION STATEMENT *(of the abstract entered in Block 20, If different from Report)*

18. SUPPLEMENTARY NOTES

19. KEY WORDS *(Continue on reverse side if necessary and identify by block number)*

graphite/epoxy composite
static strength
fatigue life
scale effect
in-series model, in-parallel model

statistical analysis

20. ABSTRACT *(Continue on reverse side if necessary and identify by block number)* The effect of size on the endurance limit of composite materials has been found to depend on the statistical scatter. For structures that can be considered as composed of a number of basic elements arranged in series, the fatigue life of the structure can be predicted if the distribution of the basic element is known. This prediction technique has been verified for graphite/epoxy structures constructed from three basic elements with central hole arranged in-series and subjected to a compression loading.

DD FORM 1473 1 JAN 73 EDITION OF 1 NOV 65 IS OBSOLETE
S/N 0102-LF-014-6601

SECURITY CLASSIFICATION OF THIS PAGE *(When Data Entered)*

NADC-78259-60

CERTIFICATION OF COMPOSITE AIRCRAFT STRUCTURES
UNDER IMPACT, FATIGUE AND ENVIRONMENTAL CONDITIONS

PART II
SCALE EFFECT IN FATIGUE OF COMPOSITE MATERIALS

by

Pei Chi Chou

Robert Croman

Drexel University
Philadelphia, Pennsylvania

2-1

January 1978

Foreword

This is part II of the final technical report for Contract No. N62269-76-C-0378, which is sponsored by the Naval Air Development Center, Warminster, Pa. The work was performed during the period of July 1, 1976 through December 30, 1977. Mr. Lee W. Gause was the contract monitor.

The contracted study is under the title "Certification of Composite Aircraft Structures under Impact, Fatigue and Environmental Conditions"; parts I and II of the study are under the supervision of Dr. P.C. Chou, while part III is under Dr. A.S.D. Wang, both of Drexel University.

This report concerns part II of the contract, the scale effect in fatigue of composite materials. It is a self-contained report including definitions of all nomenclature used, and its own introduction and conclusions.

The authors would like to thank Dr. Edward J. McQuillen, Dr. James L. Huang and Mr. Lee W. Gause for the frequent technical discussions. The authors would also like to thank Mr. James Alper and Mr. Dinh Nguyen who helped conducting the experiments.

2-II

Scale Effect in Fatigue of Composite Materials

Table of Contents

2-III

I.   Introduction

It is known that the endurance limit (fatigue limit) of a material under fatigue loading decreases as the size of the specimen increases [1]. A large amount of test data for metals are available, and many theories have been offered, but none of the theories are satisfactory. For instance, in [2] it was found that for an Al-Cu alloy the fatigue limit of a large sheet (230 mm width) is only 50% of that of a small sheet (19 mm width). In contrast, the fatigue limit for corresponding mild steel specimens showed that the large sheet has 85% the fatigue limit of the small sheet. Among factors mentioned that may contribute to the scale effect include maximum stress gradient, heating of large specimen, surface stress, etc. No statistical theory was mentioned.

Recently, the detrimental effect of size in composite material has been recognized and attempts by the statistical approach have been proposed. For instance, in Ref. [3] and [4] the ratio of strength of two specimens was assumed equal to the ratio of their volumes under stress. This, in essence, is considering that all defects or micro-flaws are arranged in series, and the weakest link breaks the chain.

The concept of in-series and in-parallel arrangement in statistical studies is not new. In classical reliability analysis the series-parallel arrangements are often used for engineering systems, see for instance Shooman [5]. These arrangements have also been assumed, sometimes implicitly, in studying the strength of structures and materials, see [6]. It seems that they have not been used to study the scale effect of fatigue life.

The goal of the present study is to obtain basic understanding of scale effect in the fatigue life of composite material structures. This basic understanding may be used to develop scaling laws such that the service life

of a full size structure may be predicted from tests of small size models or specimens.

The full size structure is considered as consisting of n "elements". These elements may be statistically in-series, or in-parallel, or a combination of these two. If the whole structure fails when any one of the elements fails, then these elements are considered to be in-series. This is also known as the weakest-link theory. On the other hand, if after one element fails, the rest of the elements can still carry the total load, the elements are considered in-parallel; this is equivalent to a bundle of loose filaments, and amenable to the bundle theory analysis.

If the strength, or fatigue life, of the element has a small statistical scatter, or large Weibull shape parameter, then the mean strength or life of the n-element structure is not too much different from that of the element. This is true for both in-series and in-parallel arrangements. However, if the scatter is large, which is the case for fatigue life of composites, the n-element structure has much shorter life than the element.

To substantiate this in-series/in-parallel model in relation to fatigue of composites, we have selected as the basic element a composite specimen with a single drilled hole, (Fig. 1). By arranging a number of holes in different arrays, we may accomplish in-series and in-parallel models. The present paper reports the results of the basic element and the three elements in-series cases, as shown in Fig. 1. This drilled-hole element was selected because it represents the rivet or bolt holes in actual structures, and it can be arranged in simple in-series/in-parallel models. Fatigue properties of riveted and bolted joints in composite panels are reported in [7] and [8].

A.   Geometry

Basic Element   3 In-Series
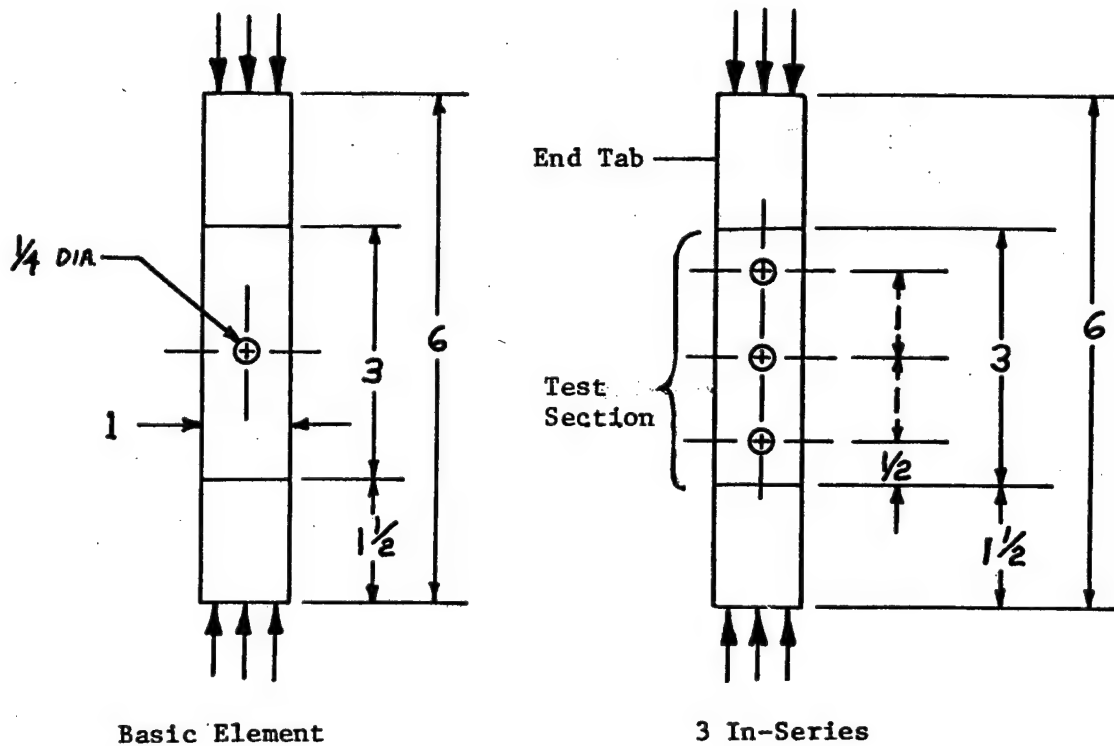
All Dimension in Inch
(1 Inch = 25.4 mm)

B.   Properties

Material: Hercules AS/3501-6 graphite epoxy

Layers: 12

Layup: $[\pm 45/0_2/\mp 45]_s$

Figure 1.   Specimen Geometry and Properties

3

The specimens were loaded in static compression and constant amplitude compression fatigue. The compression loading is used because it is known that graphite/epoxy composites have a shorter compression fatigue life as compared to tension fatigue, see Refs. [9] and [10]. The fatigue tests were at a constant amplitude of σ_{max} = 0, σ_{min} = -2800 lbf (-12.50 kN) (R = -∞). This maximum compression stress is approximately 74% of the mean static strength. Relevant properties and dimensions of the specimens are shown in Fig. 1.

The in-parallel model of scale effect is in the developement stage. Pertinent material concerning this model and its verification is contained in Appendix A.

II. Equations for the In-Series Model

In the traditional weakest link concept in material strength, the basic "link" is a flaw in the material, see for instance Ref. [11]. The present in-series model is of the same principle as the weakest link, except we use a structural "element" as a link. This element can be of a size in the same order of magnitude of the total structure. It is well-known that the weakest link concept can be described in mathematical statistics by the extreme value theory, see for instance, Ref. [12] and [13]. We shall summarize the results for elements of Weibull distribution.

Consider a basic element of Weibull distribution, with a density function

$$f(x) = \frac{\alpha (x-x_0)^{\alpha-1}}{\beta^\alpha} \exp\left[-\left(\frac{x-x_0}{\beta}\right)^\alpha\right] \tag{1}$$

and a cumulative distribution function (CDF)

$$F_X(x) = P(X \leq x) = 1 - \exp\left[-\left(\frac{x-x_0}{\beta}\right)^\alpha\right] \tag{2}$$

where x = strength or life, x_0 = position parameter, α = shape parameter, and β = scale parameter. Then the CDF of an n-element in-series specimen can be shown to be

$$F_{X_n}(x) = P(X_n \leq x) = 1 - [1 - P(X \leq x)]^n \tag{3}$$

The density function, $f_n(x)$, of the n-element specimen is then

$$f_n(x) = \frac{\alpha (x-x_0)^{\alpha-1}}{(\beta/n^{1/\alpha})^\alpha} \exp\left[-\left(\frac{x-x_0}{\beta/n^{1/\alpha}}\right)^\alpha\right] \tag{4}$$

Comparing Eq. (4) with Eq. (1), we conclude that the shape parameter α, and position parameter x_0, of the n-element in-series model are identical to those of the basic element; the scale parameter β is reduced from that of the basic element by a factor $n^{(1/\alpha)}$.

The mean strength or life is given by

$$\mu = \beta\Gamma\left(\frac{\alpha + 1}{\alpha}\right) + x_0 \qquad (5)$$

If the position parameter is equal to zero then the mean of the n-element in-series, μ_n is related to the basic element mean, μ by

$$\frac{\mu_n}{\mu} = \left(\frac{1}{n}\right)^{1/\alpha} \qquad (6)$$

The decrease of the mean is a function of the shape parameter, as well as the number of elements, n. For a value of $\alpha = 2$, the strength or life decreases a great deal; for n = 100, the strength of the in-series combination is only 10% of the basic element. For a large value of α, however, the decrease in strength is not too much. For instance, for n = 100 and $\alpha = 30$, μ_n is 86% of μ. Eq. (6) is plotted in Fig. 2.

Since for composite materials the shape parameter for static strength is between 10 to 30, and for fatigue life it is between 1 to 3, it can be seen that the size effect is more serious in fatigue life than in static strength, if the elements are in-series. In other words, a long coupon has almost the same static strength as a short element, but has only a small fraction of the fatigue life of the element.
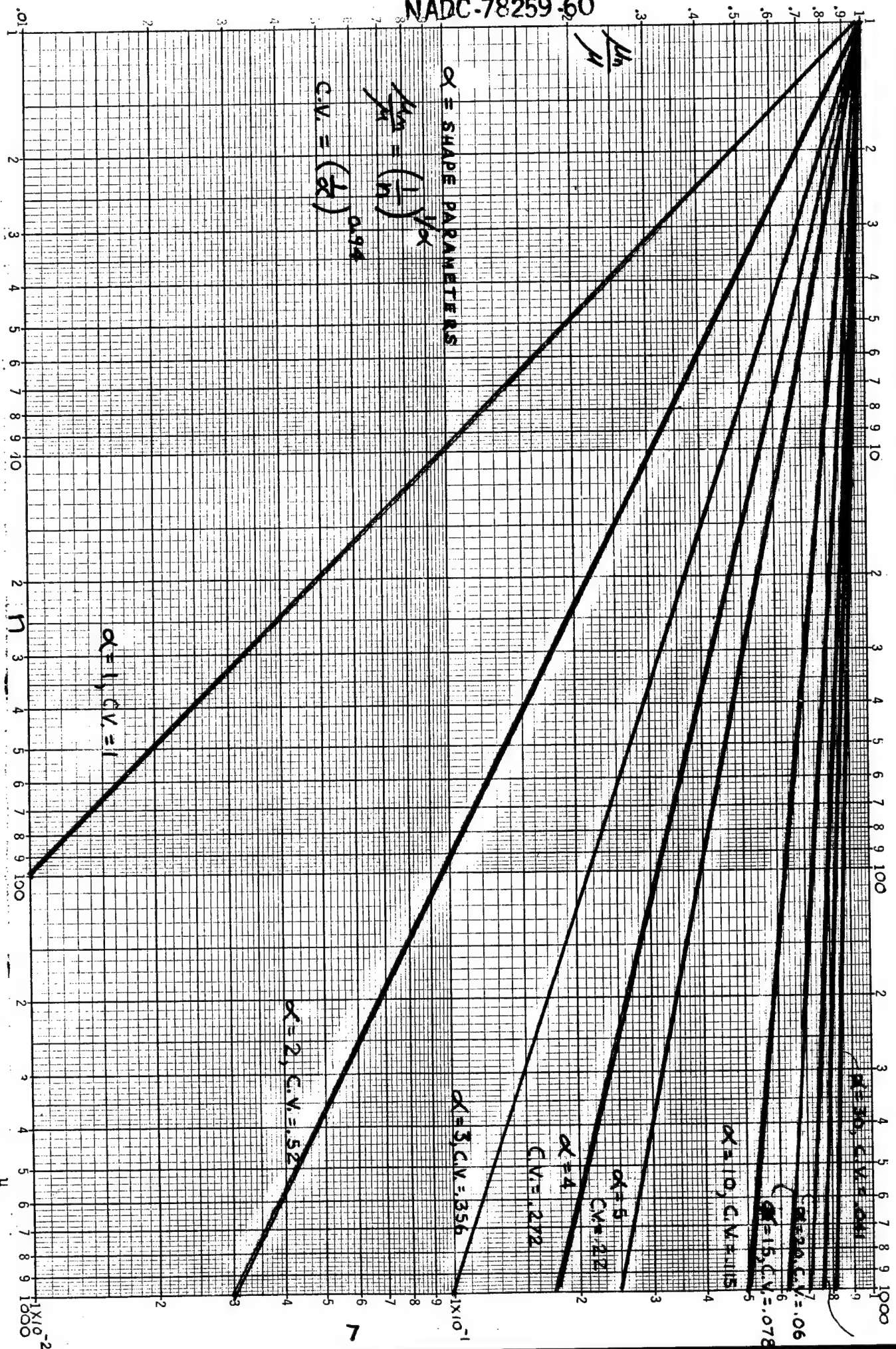
Figure 2. Ratio of Mean (of a Certain Property) of n Element in Series over the Mean of One Element vs. Number of Element, $\frac{\mu_n}{\mu}$

$\alpha = $ SHAPE PARAMETERS

$$\frac{\mu_n}{\mu} = \left(\frac{1}{n}\right)^{1/\alpha}$$

$$C.V. = \left(\frac{1}{\alpha}\right)^{0.94}$$

$\alpha = 1, C.V. = 1$

$\alpha = 2, C.V. = .52$

$\alpha = 3, C.V. = .356$

$\alpha = 4, C.V. = .272$

$\alpha = 5, C.V. = .22$

$\alpha = 10, C.V. = .115$

$\alpha = 15, C.V. = .078$

$\alpha = 20, C.V. = .06$

$\alpha = 25, C.V. = .049$

$\alpha = 30, C.V. = .041$

NADC-78259-60

K+E LOGARITHMIC
2 X 3 CYCLES
KEUFFEL & ESSER CO.
46 7320
MADE IN U.S.A.

III. Static and Fatigue Experiments

To verify the in-series model a number of static and fatigue tests were performed using both the basic element and the in-series specimen.

A. Specimens All specimens used for this study were cut from a Hercules AS/3501-6 graphite/epoxy composite plate prepared at the Naval Air Development Center, Warminster, Pa. The plate consisted of 12 layers following a layup of $[\pm 45/0_2/\mp 45]_s$. The overall measurements of the plate were 24 by 34 inches (610 by 860 mm) with an average thickness of 0.072 inch (1.83 mm). End tabs were cut from plates prepared of 3M Scotchply 1003 fiberglass/epoxy with a layup of $[0_2/90/0_2/90/0_2/90/0_2]$. The thickness of the plates were 0.080 inch (2.03 mm).

The basic element was a 1 x 6 inch (25.4x152.4 mm) strip with a central 1/4 inch (6.4 mm) hole. The in-series specimen had the same overall dimensions, but with three 1/4 inch (6.4 mm) holes. End tabs of length 1 1/2 inch (38.1 mm) were applied to the ends of both sides of each specimen, (See cutting procedure for method of application). The dimensions for the basic element and the in-series specimen are given in Fig. 1. The portion between the end tabs was considered as the test section.

The plate was cut into test specimens by means of a 5 13/16 inch (147.6 mm) diameter diamond saw blade mounted on a Sundstrand Rigidmil. The blade was run at 715 rpm with a table feed rate of 1 inch (25.4 mm) per minute. The first step in the cutting procedure consisted of cutting the plate into 6 1/2 x 10 inch (165.1x254.0 mm) sections such that the 0° fibers were parallel to the shorter edge. Next 1 1/2 x 10 inch (38.1x254.0 mm) end tab strips of 0.080 inch (2.03 mm) thickness were bonded to both sides of the sections, 1/4 inch (6.4 mm) from each of the 10 inch (254.0 mm) edges.

8

The bonding agent used was Ecobond 51 combined with Catalyst #9, both manufactured by Emerson and Cuming Inc. These sections were then squared off and cut down to 6 x 10 inch (152.4x254.0 mm) by taking off 1/4 inch (6.4 mm) along each of the 10 inch (254.0 mm) edges. Next the sections were cut into 6 x 1 inch (152.4x25.4 mm) strips. Each section yielded 9 of these strips.

Specimen holes were drilled with straight fluted solid carbide drill bits manufactured by Cleveland Twist Drill Co. First a pilot hole was made in the specimen with a 1/8 inch (3.2 mm) bit. This was enlarged with a 1/4 inch (6.4 mm) bit. The bits show no noticeable wear after drilling in excess of 200 holes.

After cutting and drilling the completed specimens were stored at room temperature and humidity until testing.

B. <u>Testing Apparatus</u> All testing was performed on an Instron Model 1230 Dynamic Test Machine equipped with a Model 836 remote control panel, a Model 602 load and stroke controller panel, and a Model 860A function generator. This testing machine has the capacity of $\pm$ 10,000 lbf ($\pm$ 40 kN) load which can be applied in the form of a sine input, triangular input, square input, or ramp input. The maximum reliable frequency for operating this machine is 30 Hz. The Instron Wedge Action Gripping Jaws were used in conjunction with our own gripping and anti-buckling guide system (to be described later). For static tests a Hewlett Packard Model 7045A X-Y Recorder was used. Additional equipment included a Tektronix 7623A Storage Oscilloscope and a Keithley Instruments 160 Digital Multimeter.

A method for gripping the specimen and for preventing buckling during loading was designed, and a sectioned assembly of this apparatus is shown in Fig. 3. As can be seen the bottom and top grips are held in place by the Instron Jaws. The gaps between the jaws and the grips are filled with shim stock. The top grip is stationary and the two vertical runners are bolted to it. The bottom grip is free to ride up and down in these runners. The applied load is transmitted by the actuator arm of the Instron through the bottom Instron Jaw to the bottom grip. The frictional force between the bottom grip and the vertical runners was found to be negligible (less than 10 lbf or 44 N). The anti-buckling guide also fits in the runners and is free to move up and down. The runners insure correct alignment of the top and bottom grips and the anti-buckling guide. Hence the test specimen will have no initial crookedness. The clearance between the anti-buckling guide faces and the specimen surfaces of course varies from specimen to specimen but on the average is 0.003 inch, (0.08 mm). The section view shows that the specimen's ends are in contact with the grip floors. This insures that the load is applied on the ends of and along the axis of the test specimen. The figure also indicates that the rear gripping plates are held in place by 1/4 20 Allen screws inserted through the front grips. The rear anti-buckling guide plate is held to the front anti-buckling guide by four screws.

Detail drawings of the grips and anti-buckling guide are presented in Appendix B.

C. <u>Testing Procedures</u> All tests were run at room temperature with ambient humidity. In order to reduce friction between the specimen and the anti-buckling guide, a thin coating of Molykote 44 grease, a heat stable silicone lubricant, was applied to the contact surfaces of the guides.
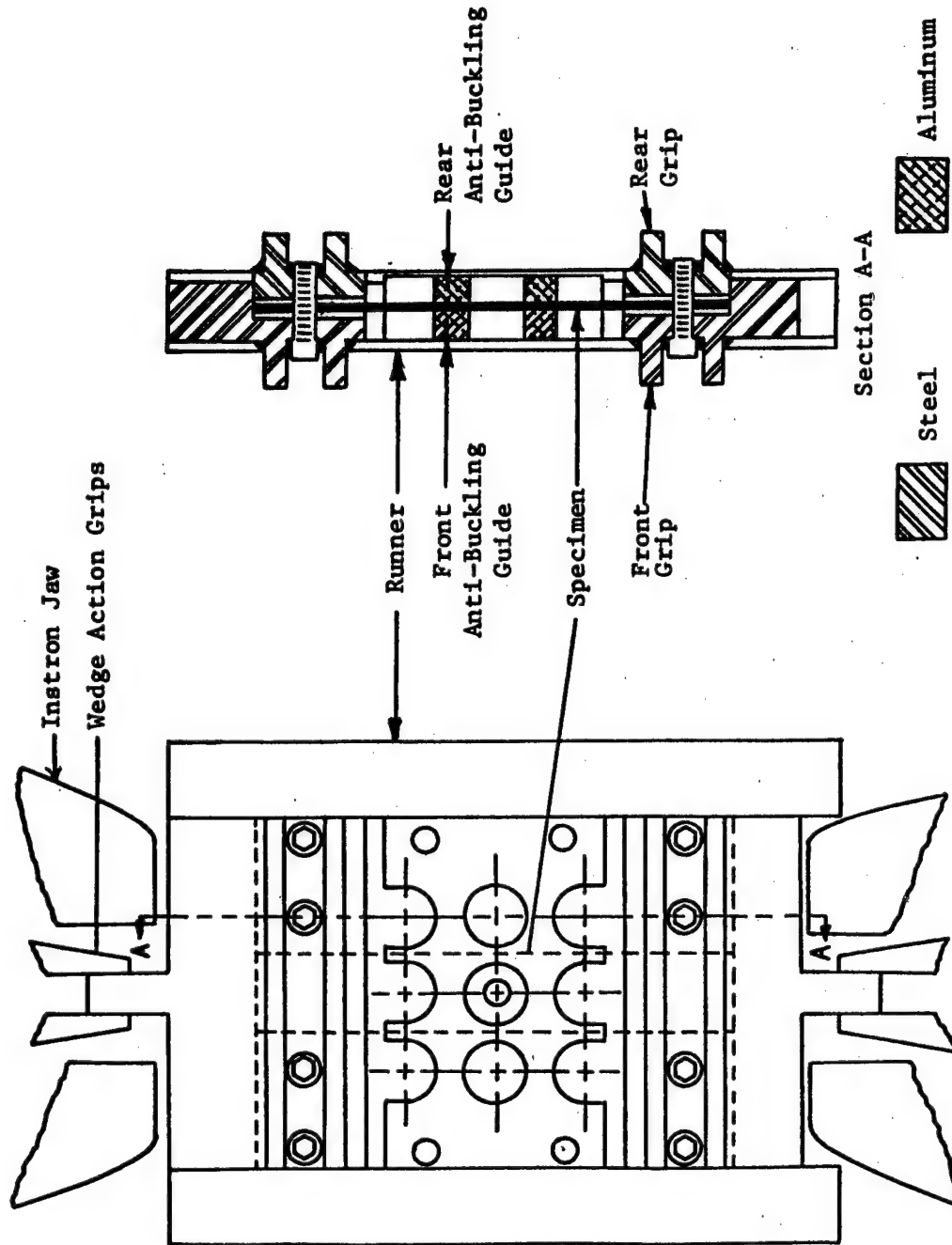
Figure 3. Sectioned Assembly, Specimen Gripping Anti-Buckling Device

For static tests the specimen was secured in the grips and the back
of the anti-buckling guide was screwed in position. A compressive load
of 10 lbf (40 N) was applied to the specimen and then the screws holding the
backs of the grips and anti-buckling guide were torqued tight. The load
was then released. Next, operating in the stroke mode and using the ramp
input a compressive load was applied to failure. The failure load was re-
corded on the X-Y plotter.

For fatigue tests, the specimen was secured in the grips and the back
of the anti-buckling guide was screwed in place (hand tight). Small
pieces of styrofoam were placed between the guide and the grips in order to
damp out any vibration. Operating in the load mode a compressive load was
gradually applied up to 100 lbf (440 N). Then the screws holding the grips
and guide in place were torqued tight. The load was then increased slowly
until the desired mean load was obtained. In the present test, the mean load
is -1400 lbf (-6.23 kN). A sine wave cycling of the applied load with an
amplitude of 1400 lbf (6.23 kN) was then started. For the first 10 cycles a
frequency of 0.01 Hz was used. During this time the loading was rechecked
with the use of the digital multimeter and oscilloscope to make sure that
the specimen did not go into tension and the load was cycling between 0 and
-2800 lbf (-12.50 kN). The frequency was then gradually and slowly increased
to 5 Hz. Periodically the loading was checked with the oscilloscope and
screws retorqued as necessary. The specimen was run to failure and fatigue
life was recorded in cycles by the control panel counter.

IV. Experimental Results

This section presents the static and fatigue test results for the basic element, the three-in-series specimen, and several other arrangements. All specimens failed through a drilled hole. For each test, the ultimate load, or the fatigue life of each specimen is given in tabular form. The sample means and sample standard deviations are also calculated from the following formulas

$$\text{Sample mean} \quad = \quad \bar{x} = \frac{1}{n} \sum_{i=1}^{n} x_i \qquad (7)$$

$$\text{Sample standard deviation} = s = \left[\frac{1}{n-1} \sum_{i=1}^{n} (x_i - \bar{x})^2 \right]^{\frac{1}{2}} \qquad (8)$$

where n is the total number of specimens tested in each case.

Table I

Static Strength and Fatigue Life of the Basic Element,
Graphite/Epoxy $[\pm 45/0_2/\overline{\mp} 45]_s$

a. Ultimate Static Compression Load, lbf (kN), (12 specimens)

2950 (13.12)	3600 (16.01)	3900 (17.35)	4350 (19.35)
3100 (13.79)	3630 (16.15)	3900 (17.35)	4600 (20.46)
3250 (14.46)	3770 (16.77)	3940 (17.55)	4650 (20.68)

$$\bar{x} = 3800 \ (16.90)$$
$$s = 550 \ (2.45)$$

b. Compression Fatigue Life, Cycles, Max. Compression Load = 74% Basic Element Mean Static Strength, R = -∞, Frequency = 5 Hz (10 specimens)

17230	26230	78750	107880	127540
20010	49460	83300	112120	128780

$$\bar{x} = 75130$$
$$s = 44200$$

13

Table Ia presents the static strength measured in lbf (kN) for the basic elements. The sample mean and sample standard deviation are 3800 and 550 lbf (16.90 and 2.45 kN) respectively. Table Ib gives the fatigue life measured in cycles for the basic elements. The maximum compressive load to which each element was subjected was 2800 lbf (74% of mean static) while the minimum load was 0. The mean and standard deviation of the basic element fatigue life were 75,130 and 44,200 cycles respectively.

Table II

Static Strength and Fatigue Life of the Three-In-Series Specimen, Graphite/Epoxy $[\pm 45/0_2/\mp 45]_s$

a. Ultimate Static Compression Load, lbf (kN), (10 specimens)

3000 (13.34)T*	3260 (14.50)T	3450 (15.35)B	3660 (16.28)B
3150 (14.01)B	3400 (15.12)B	3600 (16.01)B	
3150 (14.01)T	3400 (15.12)M	3600 (16.01)T	

$$\bar{x} = 3370 \ (14.99)$$
$$s = 220 \ (1.00)$$

b. Compression Fatigue Life, Cycles, Max. Compression Load = 74% Basic Element Mean Static Strength, R = $-\infty$, Frequency = 5 Hz (9 specimens)

2090 M	15270 B	19990 M	29950 M	47690 B
5040 T	16090 B	24700 B	32740 B	

$$\bar{x} = 21510$$
$$s = 14200$$

* Failed hole location, T = top, M = middle, B = bottom.

Table IIa shows the static strength measured in lbf (kN) for the three-in-series specimens. Also the position of the failure is given. The sample mean is 3370 lbf (14.99 kN) and the standard deviation is 220 lbf (1.00 kN). Table IIb presents the fatigue life in cycles and the position of the failed hole for each of the three-in-series specimens subjected to the same loading conditions as the basic element fatigue specimens. Here, $\bar{x} = 21,510$ cycles, and s = 14,200 cycles.

We see that in the static case the mean strength of three-in-series specimen is 89% of the basic element mean strength. However, the mean life of the three-in-series specimen is 29% of the basic element mean life. It is evident that the in-series configuration greatly reduces the fatigue life, but has a much less effect on the static strength.

Some additional tests were performed on specimens with different geometries than described above. This data is compiled in Appendix C.

V. Parameter Estimations

A. Interval Estimation for the Mean

According to the in-series model, the life and strength of the three-in-series specimen should be lower than those of the basic element. From the data in the previous section, it can be seen that indeed the sample mean life and mean strength for the three-in-series are both lower than the corresponding basic element values. The sample mean values, however, are random variables, dependent on the sample size, and by themselves have less statistical significance. In order to establish a confidence level on the hypothesis that the three-in-series and basic element specimens were from two different populations and that the three-in-series case has a lower mean value, we shall make interval estimations for the means.

We shall assume that the random variable

$$t_{n-1} = \frac{(\bar{x}-\mu)\sqrt{n}}{s} \tag{9}$$

has the Student-t distribution with n-1 degree of freedom. Strictly speaking, this is true only when the population is normal. For practical purposes, it is a good enough approximation for non-normal distributions, [14]. Based on this assumption, we have estimated the confidence intervals for all four cases, and listed the results in Table III.

Table III

Confidence Intervals for Basic and Three-In-Series Specimens

.. Fatigue Life

Specimen	Confidence Interval for Mean Life, Cycles	% Confidence
Basic	[43510, 106750]	95%
3-in-series	[10600, 32420]	95%

b. Static Strength

Specimen	Confidence Intervals for Mean Strength		% Confidence
	lbf	kN	
Basic	[3520, 4090]	[15.7, 18.2]	90%
	[3460, 4150]	[15.4, 18.5]	95%
Three-in-series	[3240, 3500]	[14.4, 15.6]	90%
	[3200, 3530]	[14.3, 15.7]	95%

As can be seen the 95% confidence intervals of the population mean lives of the basic element and three-in-series specimen are disjoint, and the former larger than the latter. This implies that these sample means come from separate populations and the basic element has longer life. Table III also lists the 90% and 95% confidence intervals for the basic and three-in-series mean strengths. Here it is seen that the 95% confidence intervals overlap whereas the 90% intervals do not. It can be argued, although not as strongly as in the fatigue case, that the strength results of the basic and three-in-series elements do indeed come from different populations.

B. Point Estimation, Weibull Distribution

It is well-known that the strength and fatigue life of materials can be best characterized by the log-normal or the Weibull distributions. In this study, the two parameter Weibull distribution is used to represent our results. The cumulative distribution function (CDF) has the form,

$$F(x) = P(X \leq x) = 1 - \exp\left[-\left(\frac{x}{\beta}\right)^{\alpha}\right] \qquad (10)$$

Having collected sample points x, the parameters can be estimated in many ways, for instance, method of moments, maximum likelihood, and regression. In this study the method of linear regression was used to estimate α and β. This technique requires an assignment of numerical values of P_i (called the rank) for each x_i. There are many ways of making this assignment but in this study the median rank method was used. Here the sample points are ordered from lowest to highest and then P_i is assigned by the approximate median rank formula

$$P_i = \frac{i - 0.3}{n + 0.4}, \quad i = 1,\ldots,n \qquad (11)$$

where n is the total number of data points comprising the sample.

In using linear regression, let us transform Eq. (10), by taking the logarithm twice, into the form

$$y' = \alpha x' - \alpha \ln \beta \qquad (12)$$

where

$$x' = \ln x \qquad (13)$$

$$y' = \ln \ln \left[\frac{1}{1-P(X \leq x)}\right]. \qquad (14)$$

At $x = x_i$, the corresponding values of x_i' and y_i' can be evaluated from Eqs. (13) and (14). The quantity y_i' is associated with the theoretical distribution (10), evaluated at x_i. The corresponding value from the approximate rank is given by

$$y_i = \ln \ln \left[\frac{1}{1-P_i}\right] \qquad (15)$$

The difference $y_i - y_i'$, which represents the error, is squared, and summed over i or,

$$\Delta^2 = \sum_{i=1}^{n} (y_i - y_i')^2$$

$$= \sum_{i=1}^{n} (y_i - \alpha x_i' - \alpha \ln \beta)^2$$

(16)

This sum of the square of errors is then minimized, by forming the two equations $\partial \Delta^2 / \partial \alpha = 0$ and $\partial \Delta^2 / \partial \beta = 0$. Solving these two equations yields the two unknown parameters as

$$\alpha = \frac{\sum\limits_{i=1}^{n} x_i y_i - \frac{1}{n} \sum\limits_{i=1}^{n} x_i \sum\limits_{i=1}^{n} y_i}{\sum\limits_{i=1}^{n} x_i^2 - \frac{1}{n} \left(\sum\limits_{i=1}^{n} x_i \right)^2}$$

(17)

$$\beta = \exp \left[\frac{\alpha \sum\limits_{i=1}^{n} x_i - \sum\limits_{i=1}^{n} y_i}{n \alpha} \right]$$

(18)

Table IV gives the values of α and β for the four cases. Values of the mean μ and coefficient of variation are also listed and were obtained from the formulas

$$\mu = \beta \Gamma \left(\frac{\alpha+1}{\alpha} \right)$$

(19)

$$\text{C.O.V.} = \left[\frac{\Gamma \left(\frac{\alpha+2}{\alpha} \right) - \Gamma^2 \left(\frac{\alpha+1}{\alpha} \right)}{\Gamma^2 \left(\frac{\alpha+1}{\alpha} \right)} \right]^{1/2}$$

(20)

19

Table IV

Estimated Weibull Parameters for
Basic Element and Three-In-Series Specimens

a. Fatigue-Life, cycles

Specimen	α	β cycles	μ cycles	C.O.V.
Basic Element	1.36	87840	80400	.74
Three-in-series	1.09	25390	24700	.93

b. Static Strength, lbf (kN)

Specimen	α	β lbf (kN)	μ lbf (kN)	C.O.V.
Basic Element	7.6	4040 (17.97)	3800 (16.90)	.15
Three-in-series	16.2	3470 (15.44)	3360 (14.95)	.06

The Kolmogorov-Smirnov goodness of fit test was used to see how well
the Weibull distributions described the data. In all cases the fitted
distributions were acceptable at a significance level of 5%.

Fig. 4 presents the Weibull CDF for the fatigue life. The solid
curve represents the CDF for the basic element and the dashed curve the three-
in-series. The ten data points for the basic element are plotted as x's
and the nine data points for the three-in-series are given as open circles.
It can be seen that the scatter for both the basic element and three-in-
series specimen is large. The Weibull distributions fit the data points
fairly well.

Fig. 5 shows the CDFs and data points for the static strength. Once
again the solid curve and x's are for the basic element; the dashed curve
and open circles give the three-in-series information. The static strength
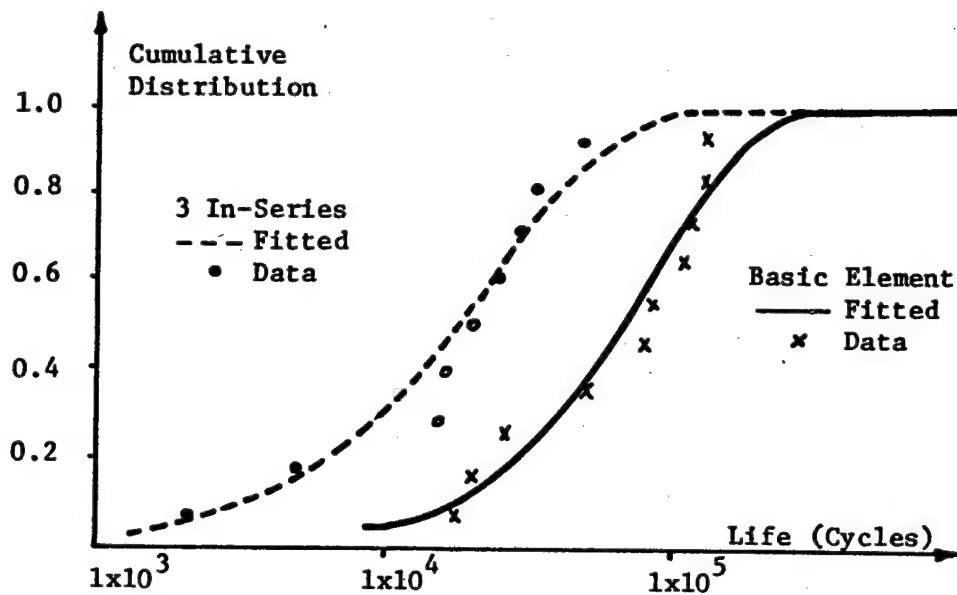is seen to have much less scatter than the fatigue life.

Figure 4 Distribution Curves for Compression Fatigue
Data of Graphite/Epoxy Max. Compressive Load
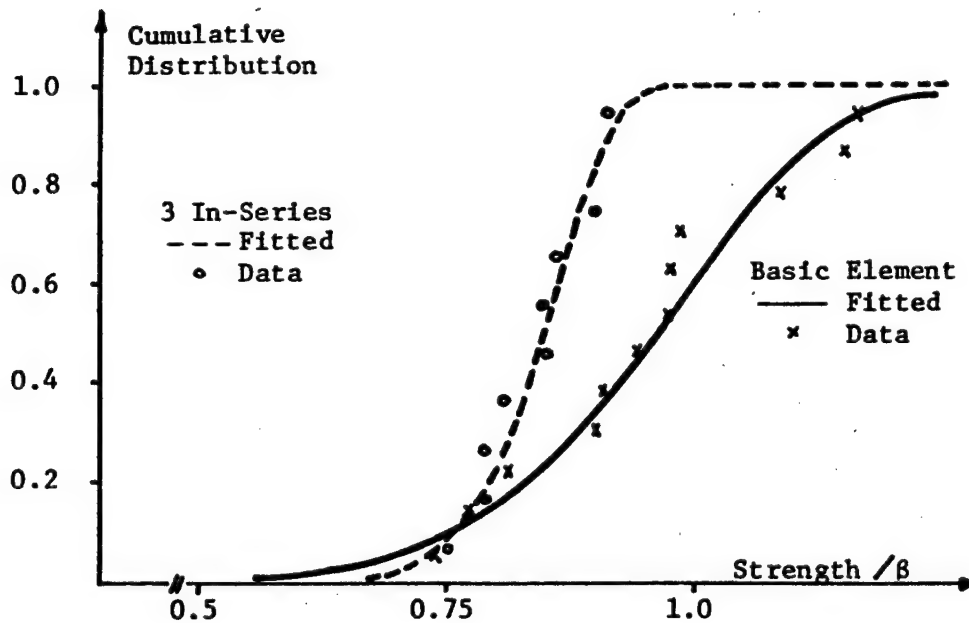= 74% Basic Element Mean Strength

Figure 5 Distribution Curves for Static Compression Strength
Data of Graphite/Epoxy.
β, Basic Element Scale Parameter = 4040 lbf (17.97 kN)

21

Looking at the estimated population means we find that the static strength of the three-in-series specimen is 89% of that of the basic element. However, the fatigue life of the three-in-series is only 31% of the basic element. These percentages are seen to be in general agreement with those discussed in the previous section that were calculated from the sample means.

VI. Analysis and Conclusions

From the theoretical analysis, it can be seen that once the distribution of the basic element, Eq. (2) is known, the distribution of the in-series specimen can be calculated from Eq. (3). This is done for both the static strength and the fatigue cases, and the results are presented in Table V. They are also shown in graphical form in Figs. 6 and 7. The calculated ones are labeled "predicted", while the fitted experimental ones are labeled "experimental".

Table V

Comparison of Measured and Predicted Properties
of Three In-Series Model

a. Fatigue Case (Large scatter, small shape parameter).

	Basic Element	Three in series	
		Predicted	Measured
Shape Parameter	1.36	1.36	1.09
Mean Life cycles	80400	35900	24700

b. Static Case (Small scatter, large shape parameter)

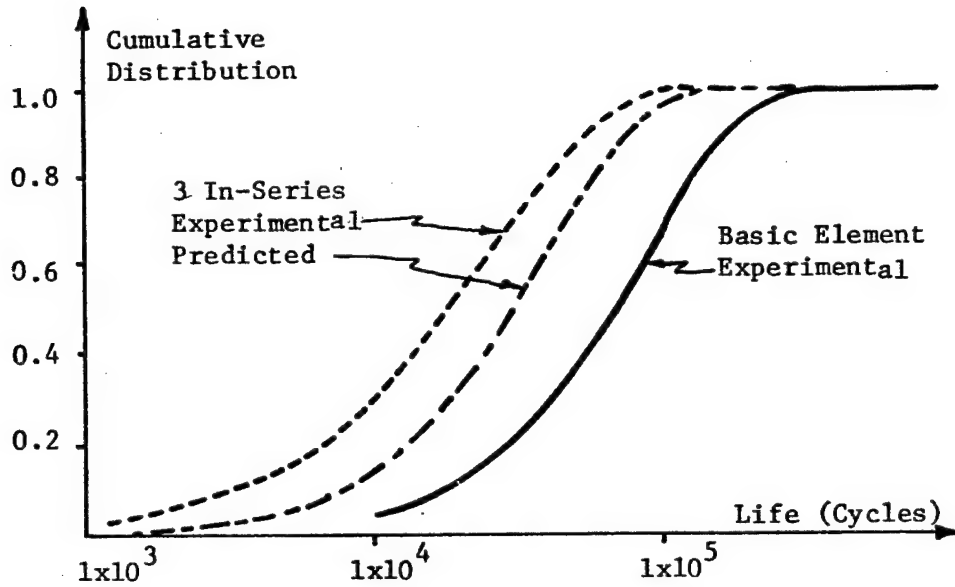|	Basic Element	Three in series	
		Predicted	Measured
Shape Parameter	7.6	7.6	16.2
Mean Strength lbf (kN)	3800 (16.90)	3290 (14.63)	3360 (14.95)

Figure 6   Predicted and Measured Distribution Curves
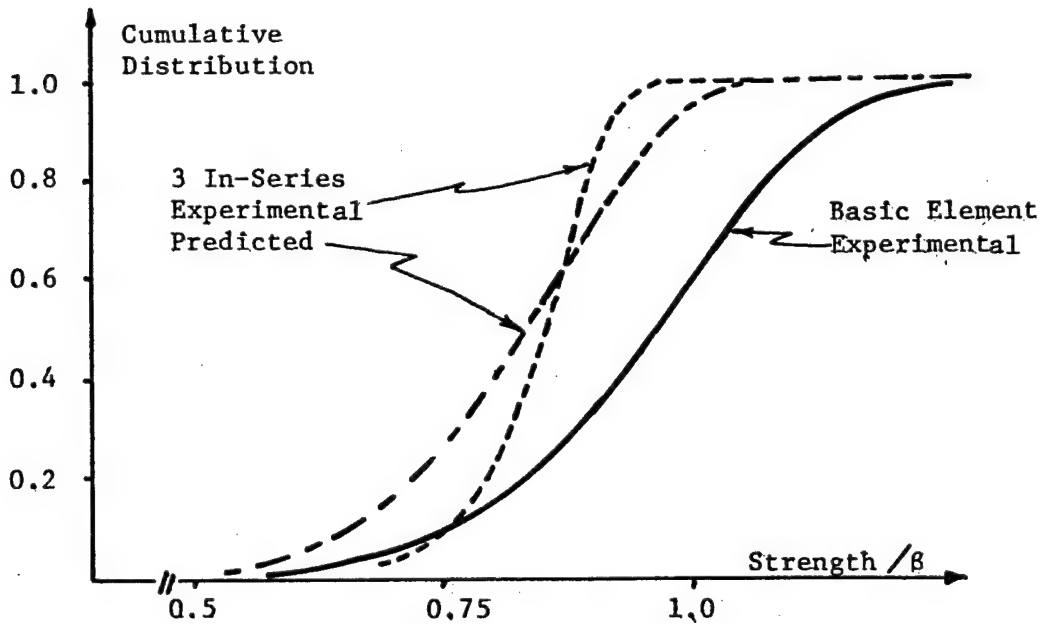for Compression Fatigue of Graphite/Epoxy.

Figure 7   Predicted and Measured Distribution Curves for
Static Compression Strength of Graphite/Epoxy
β, Basic Element Scale Parameter = 4040 lbf (17.97 kN)

For the life of the three-in-series specimen we see from Fig. 6 that the shapes of the experimental curve and predicted one are close; however the predicted mean life is 45% higher than the experimental. One possible explanation for this is that the stress distribution is non-uniform along the length of the specimen and the bottom hole is subjected to higher load, and therefore has shorter life than the other two. This is born out by the fact that in the three-in-series fatigue case over 50% of the specimens failed at the bottom hole.

In the case of the static strength the shapes of the experimental and predicted are different, but the mean strengths agree to within 3%.

Based on the results and analysis presented in this report the following conclusions can be drawn,

A.   The statistical scatter of strength and life of a basic element is one of the main reasons for the decrease in strength and life for larger structures. In other words, the scale effect in fatigue can be explained by statistical considerations.

B.   In general, a large structure contains many small elements which are statistically arranged in a combination of in-series and in-parallel modes. For certain special structures, a simple in-series arrangement can be assumed. In the present case, the three-holed specimen is truly an in-series model, and its life and strength calculated from theory are in good agreement with measured data.

C.   The larger the scatter of the strength or life among specimens, or the smaller the Weibull shape parameter, the larger their decrease for large structures due to the scale effect. Since in general there is more scatter in fatigue life than in static strength, the scale effect is more pronounced in fatigue. It is also observed that there is more scatter in fatigue life

for graphite composite materials than for metals. Consequently, fatigue
data obtained from small composite coupons must be used with caution
when applied to larger structures.

Nomenclature

CDF	Abbreviation standing for cumulative distribution function
C.O.V.	Coefficient of Variation
$f(x)$	Probability density function
F	Force applied to a bundle of fibers
F_τ	Breaking force of a bundle of fibers
$F(x)$	Cumulative distribution function
n	Number of fibers or elements (as a subscript – the number of elements in series; as a super script in parenthesis – the number of elements or fibers in parallel). Also total number of data points in a sample.
n'	Number of surviving fibers or elements
$P(X \leq x)$	Cumulative distribution function
P_i	Median rank
s	Sample standard deviation
x	Value of strength or life
x_0	Position parameter
$\bar{x}$	Sample mean
x_τ	Value of breaking force of a fiber
X	Strength or life of a basic element
X_n	Strength or life of an n in-series element
$X^{(n)}$	The failure load of the bundle/n.
α	Weibull shape parameter
β	Weibull scale parameter
σ	Population standard deviation
μ	Population mean

27

References

1. Heywood, R.B., Designing Against Fatigue of Metals, Chapman & Hall, Ltd., London, 1962.

2. Phillips, C.E., and Fenner, A.J., "Some Fatigue Tests on Aluminum Alloy and Mild Steel Sheet, with and without Drilled Holes," Proc. IME, 165, WEP 65 1951, 125-40.

3. Halpin, F.C., Gerina, K.L., and Johnson, T.A., "Characterization of Composites for the Purpose of Reliability Evaluation," AFML-TR-72-289, Air Force Material Lab., Dec. 1972.

4. Bullock, R.E., "Strength Ratios of Composite Materials in Flexure and in Tension," J. Comp. Materials, Vol. 8, p. 200, April 1974.

5. Shooman, M.L., Probabilistic Reliability - An Engineering Approach, McGraw-Hill, New York, 1968.

6. McCarthy, J.F., and Orringer, O., "Some Approaches to Assessing Failure Probabilities of Redundant Structures," in Composite Reliability, ASTM Special TP 580, Phila., 1975, pp. 5-31.

7. Wolff, R.V., and Lemon, G.H., "Reliability Prediction for Composite Joints - Bonded and Bolted," Technical Report AFML-TR-74-197, by General Dynamics, Fort Worth, for AFML Wright-Patterson AFB, Ohio, March, 1976.

8. Eggwertz, Sigge, "Investigation of Fatigue Life and Residual Strength of Wing Panel for Reliability Purposes," in Probabilistic Aspects of Fatigue, edited by R.A. Heller, ASTM STP 511, Phila., Pa. 1972, pp. 75-105.

9. Rosenfeld, M.S., and Huang, S.L., "Fatigue Characteristics of Graphite/Epoxy Laminates under Compression Loading," Proceedings of AIAA/ASME 18th Structures, Structural Dynamics and Materials Conf., March, 1977, San Diego, Vol. A., pp. 423-427.

10. Haskins, J.F., Kerr, J.R., and Stein, B.A., "Flight Simulation Testing of Advanced Composites for Supersonic Cruise Aircraft Applications," Proceedings of AIAA/ASME 18th SDM Meeting, Vol. A., March 1977, pp. 236-245.

11. Gücer, D.E. and Gurland, J., "Comparison of the Statistics of Two Fracture Modes," J. Mech. Phys. Solids, Vol. 10, 1962, pp. 365-373.

12. Epstein, B., "Statistical Aspects of Fracture Problems," Jour. Applied Physics, Vol. 19, Feb. 1948, pp. 140-147.

13. Mann, N.R., Schafer, R.E., and Singpurwalla, N.D., Methods for Statistical Analysis of Reliability and Life Data, John Wiley and Sons, New York, 1974.

14. Guttman, I., Wilks, S.S., and Hunter, J.S., Introductory Engineering Statistics, John Wiley and Sons, New York, 1971.

15. Daniels, H.E., "The Statistical Theory of the Strength of Bundles of Threads. I," Proceedings of the Royal Society of London, Ser. A, Vol. 183, June, 1945.

Appendix A   The In-Parallel Model – Bundle Theory

   The in-parallel model of scale effect considers a number of basic ele-
ments (fibers) arranged in parallel so that if one or more break, the sur-
vivors will carry a redistributed load. The theory for this model is based
on the bundle theory of Daniels [15]. The model is applicable to both the
static and fatigue modes of loading. However the existing set of equations
of the bundle theory can be applied only to the static case and is reported
in this appendix. In order to apply the bundle theory to the fatigue case,
additional development is needed.

The Exact Formula   The cumulative distribution function (CDF) of the fiber
under a static load is

$$F_X(x) = P(X \le x) \tag{A-1}$$

where X is the breaking load of the fiber. Grouping n fibers together in
parallel will form a bundle. If this bundle is subjected to a static loading
and if after any fiber failure the survivors share the load evenly then the
distribution of the bundle is

$$F_{X^{(n)}}(x) = P(X^{(n)} \le x) = \sum_{m=1}^{n} \sum_{r} (-1)^{n-m} n! \left[P\left(X \le \frac{nx}{r_1}\right) \right]^{r_1}$$

$$\left[P\left(X \le \frac{nx}{r_1+r_2}\right) \right]^{r_2} \cdots \left[P(X \le x) \right]^{r_m} \bigg/ r_1! r_2! \cdots r_m! \tag{A-2}$$

where $X^{(n)}$ = the failure load of the bundle/n. The r_i's are integers
greater than or equal to one such that

$$\sum_{i=1}^{m} r_i = n \tag{A-3}$$

where $0 < m \le n$. The inner sum in Eq. (A-2) indicates the sum over all

29

combinations of r_i subject to the condition given in Eq. (A-3).

For two fibers arranged in parallel Eq. (A-1) reduces to

$$P(X^{(2)} \leq x) = 2P(X \leq 2x)P(X \leq x) - [P(X \leq x)]^2 \qquad (A-4)$$

As the number of elements or fibers increases Daniels' exact formula quickly becomes unmanageable. We have expanded Eq. (A-2) for values of n up to n=7. For the case of n=7 the expression contains 64 terms. The expanded formulas and the associated computer program listing are given at the end of this appendix. However, as the number of elements becomes large, $P(X^{(n)} \leq x)$ approaches a normal distribution and its mean can be expressed in a simple formula. This will be derived below.

The Large Bundle Theory   The large bundle theory, which was presented by Daniels, can be derived by simple considerations. The result is limited, however, to the mean strength of the bundle. The standard deviation of the normally distributed strength was given by Daniels after a lengthy statistical derivation. In the following, we shall derive the mean strength expression and present Daniels' standard deviation formula without derivation.

Consider a bundle of fibers subjected to a force F. Each fiber will experience a force x where

$$x = \frac{F}{n'} \qquad (A-5)$$

and n' is the total number of surviving fibers currently in the bundle.

Let the probability that a single fiber breaks under the force x be $P(X \leq x)$,

$$P(X \leq x) = \int_0^x f(\zeta)d\zeta \qquad (A-6)$$

where $f(\zeta)$ is the probability density function.

30

The reliability is given by

$$R(x) = 1 - P(X \leq x) = \int_{x}^{\infty} f(\zeta)d\zeta \qquad (A-7)$$

The total number of fibers surviving will be n',

$$n' = n\,R(x) = n[1 - P(X \leq x)] \qquad (A-8)$$

where n is the total number of fibers originally in the bundle.

The relationship between the force applied to the bundle, the force experienced by each surviving fiber, and the number of original fibers is obtained by substituting Eq. (A-8) into Eq. (A-5) and rearranging, or,

$$F = n\,x[1 - P(X \leq x)] \qquad (A-9)$$

The breaking load F_τ can be obtained by maximizing the force F in Eq. (A-9); this yields

$$\frac{dF}{dx} = 0$$

or

$$\frac{d}{dx}\{nx[1 - P(X \leq x)]\} = 0 \qquad (A-10)$$

Performing the differentiation yields the equation

$$[1 - P(X \leq x)] = x\,f(x) \qquad (A-11)$$

The value of x that solves Eq. (A-11) will be designated as x_τ. The corresponding value of the breaking load is obtained by substituting x_τ into Eq. (A-9). Thus

$$F_\tau = n\,x_\tau[1 - P(X \leq x_\tau)] \qquad (A-12)$$

Daniels shows that large bundles have failure strength that are of a normal (or standard) distribution. The mean strength $\mu^{(n)}$ is then given by F_τ/n, and the standard deviation is

$$\sigma^{(n)} = x_\tau \sqrt{\frac{P(X \leq x_\tau)[1 - P(X \leq x_\tau)]}{n}} \qquad (A-13)$$

When a Weibull distribution is assumed for the single fiber, the value of x_τ can readily be obtained from Eq. (A-11). The Weibull density and distribution functions are

$$f(x) = \frac{\alpha(x-x_0)^{\alpha-1}}{\beta^\alpha} \exp\left[-\left(\frac{x-x_0}{\beta}\right)^\alpha\right] \qquad (A-14)$$

and

$$P(X \leq x) = 1 - \exp\left[-\left(\frac{x-x_0}{\beta}\right)^\alpha\right] \qquad (A-15)$$

We will further assume $x_0 = 0$.

Substituting the Weibull distribution into Eq. (A-11) and solving gives x_τ

$$x_\tau = \frac{\beta}{(\alpha)^{1/\alpha}} \qquad (A-16)$$

The breaking force from Eq. (A-12) will therefore be

$$F_\tau = n \frac{\beta}{(\alpha)^{1/\alpha}} \exp\left(-\frac{1}{\alpha}\right) \qquad (A-17)$$

Then for large bundles, the mean and standard deviation will be

$$\mu^{(n)} = \frac{\beta}{(\alpha)^{1/\alpha}} \exp\left(-\frac{1}{\alpha}\right) \qquad (A-18)$$

and

$$\sigma^{(n)} = \frac{\beta}{\alpha^{1/\alpha}} \sqrt{\frac{[1 - \exp(-\frac{1}{\alpha})]\exp(-\frac{1}{\alpha})}{n}} \qquad (A-19)$$

The coefficient of variation, C.O.V., is just the ratio of σ to μ. Therefore for a large bundle

$$\text{C.O.V.}^{(n)} = \left[\frac{[1 - \exp(-\frac{1}{\alpha})]}{n \exp(-\frac{1}{\alpha})}\right]^{1/2} \tag{A-20}$$

As can be seen the mean strength is independent of the number of fibers (or elements) arranged in parallel whereas $\sigma^{(n)}$ and $\text{C.O.V.}^{(n)}$ are inversely proportional to the square root of n.

Figures A-1-3 show the CDF of the bundle where the basic elements are Weibull with indicated shape parameter. The distributions for n = 2,3,4, 5,6,7,50,100, and 1000 elements in parallel plus the basic element are shown. Values of shape parameter of the basic element used are 2,14, and 24. The plots have been nondimensionalized by the scale parameter of the basic element. Also tabulated on these figures are the values of μ/β, σ/β, and C.O.V. for each arrangement.

Interpolation for n=7 to 50   For small values of n, up to n=7, we have expanded and calculated the exact bundle formula. For large values of n, the large bundle equations are applicable. There is a need to have formulas for the intermediate range of n, say, between n=7 and 50. We shall attempt to do this by interpolation. Figure A-4 is a plot of the mean strength for both large bundles and small bundles. The values for n=7 to 50 can be interpolated as shown. Similarly, Fig. A-5 shows the corresponding plots for the coefficient of variation.

Planned Experimental Work   In our experimental program, we intend to test Daniels' formula for three elements in parallel subjected to a static load.

n	$\frac{\mu}{\beta}$	$\frac{\sigma}{\beta}$	c.o.v.
1	0.886	0.464	0.524
2	0.720	0.284	0.395
3	0.650	0.222	0.342
4	0.611	0.188	0.307
5	0.585	0.164	0.282
6	0.567	0.149	0.262
7	0.554	0.136	0.246
50	0.429	0.049	0.114
100	0.429	0.035	0.081
1000	0.429	0.011	0.025

$\alpha = 2$, Basic Element Shape Parameter

$\beta = $ Basic Element Scale Parameter
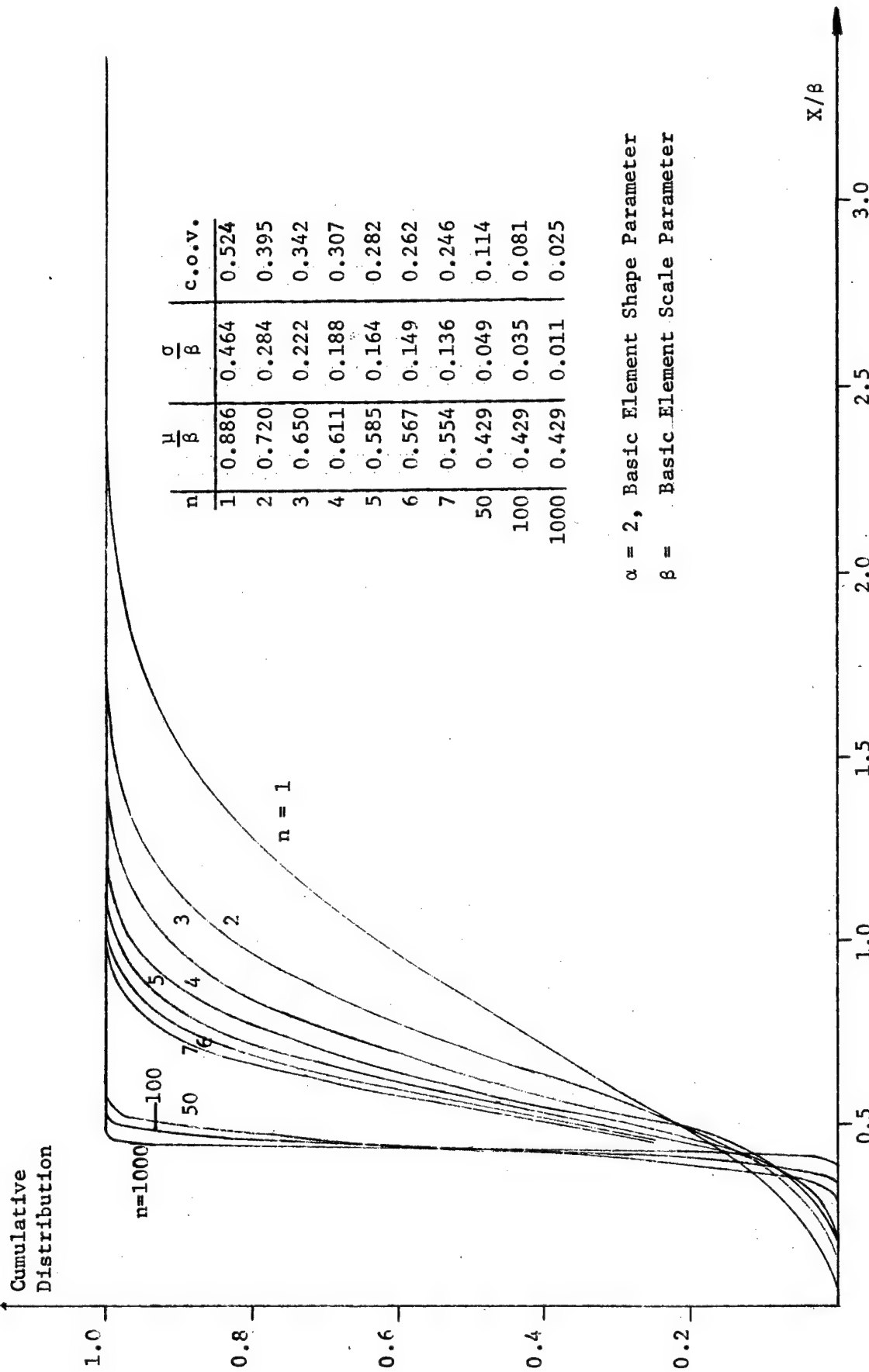
Figure A-1 Distribution Curves of n Basic Elements in Parallel
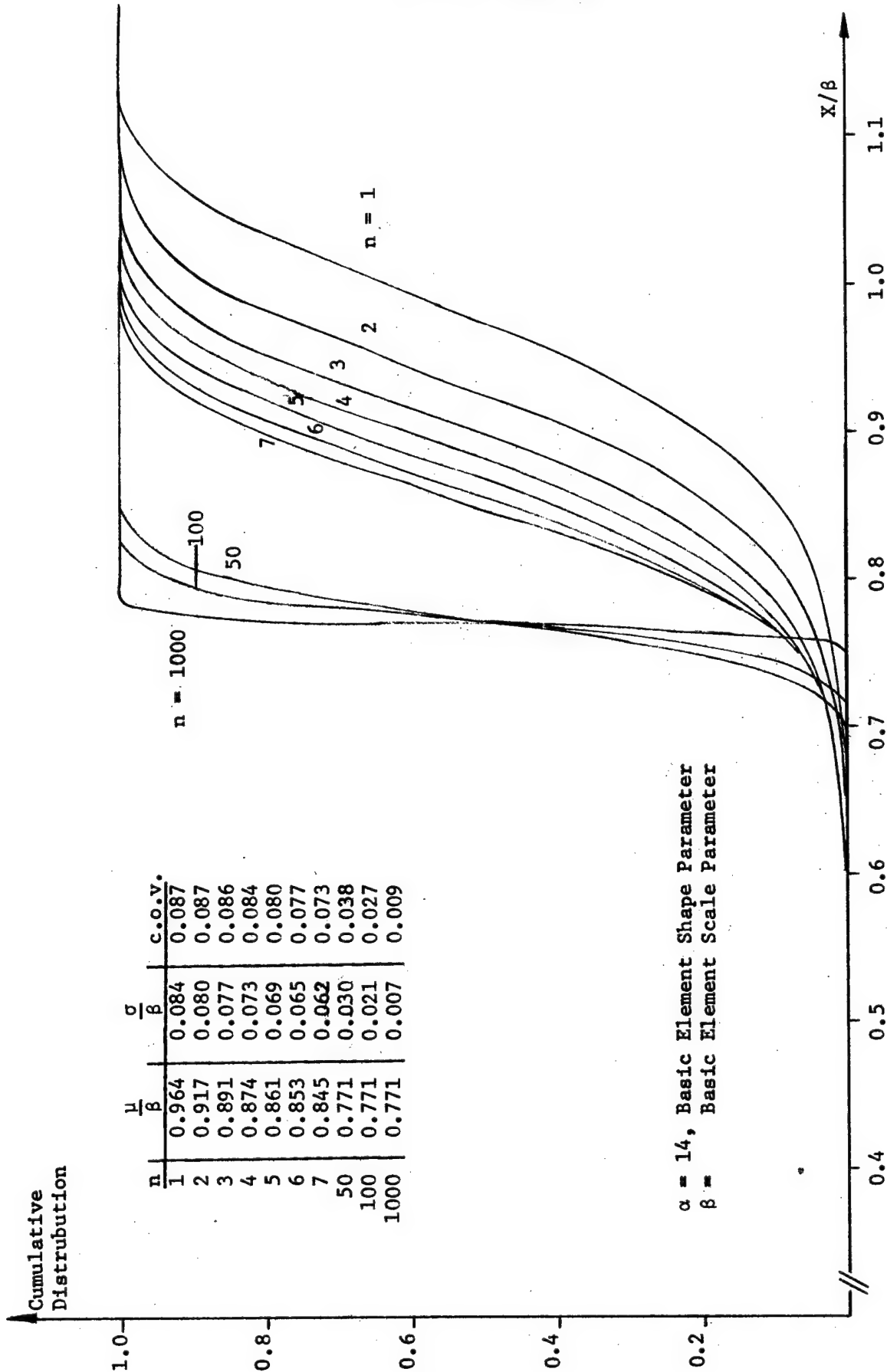
Figure A-2 Distribution Curves of n Basic Elements in Parallel

n	$\frac{\mu}{\beta}$	$\frac{\sigma}{\beta}$	c.o.v.
1	0.964	0.084	0.087
2	0.917	0.080	0.087
3	0.891	0.077	0.086
4	0.874	0.073	0.084
5	0.861	0.069	0.080
6	0.853	0.065	0.077
7	0.845	0.062	0.073
50	0.771	0.030	0.038
100	0.771	0.021	0.027
1000	0.771	0.007	0.009

α = 14, Basic Element Shape Parameter
β = Basic Element Scale Parameter
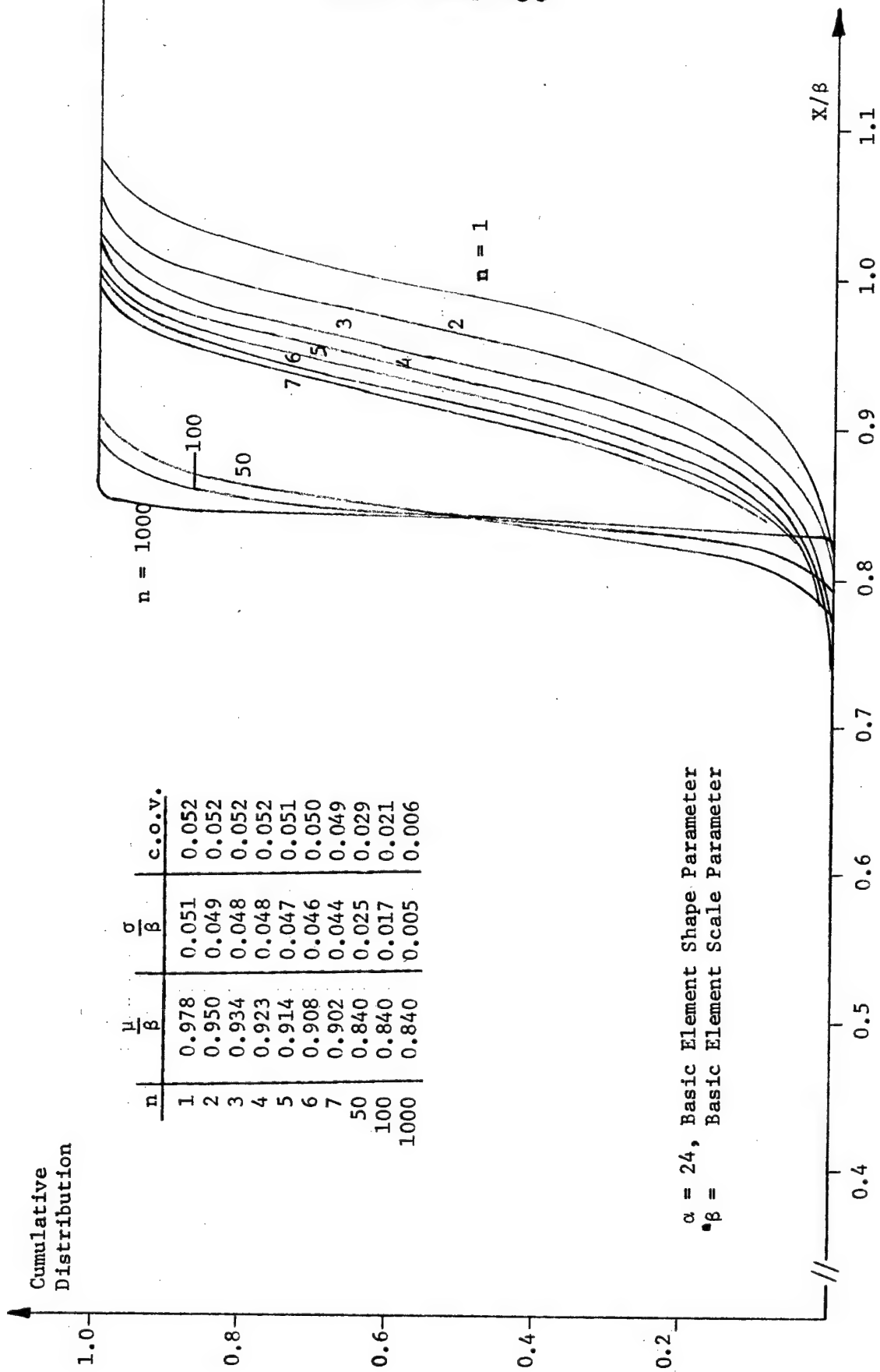
Figure A-3 Distribution Curves of n Basic Elements in Parallel

Cumulative Distribution

n	$\frac{\mu}{\beta}$	$\frac{\sigma}{\beta}$	c.o.v.
1	0.978	0.051	0.052
2	0.950	0.049	0.052
3	0.934	0.048	0.052
4	0.923	0.048	0.052
5	0.914	0.047	0.051
6	0.908	0.046	0.050
7	0.902	0.044	0.049
50	0.840	0.025	0.029
100	0.840	0.017	0.021
1000	0.840	0.005	0.006

$\alpha = 24$, Basic Element Shape Parameter
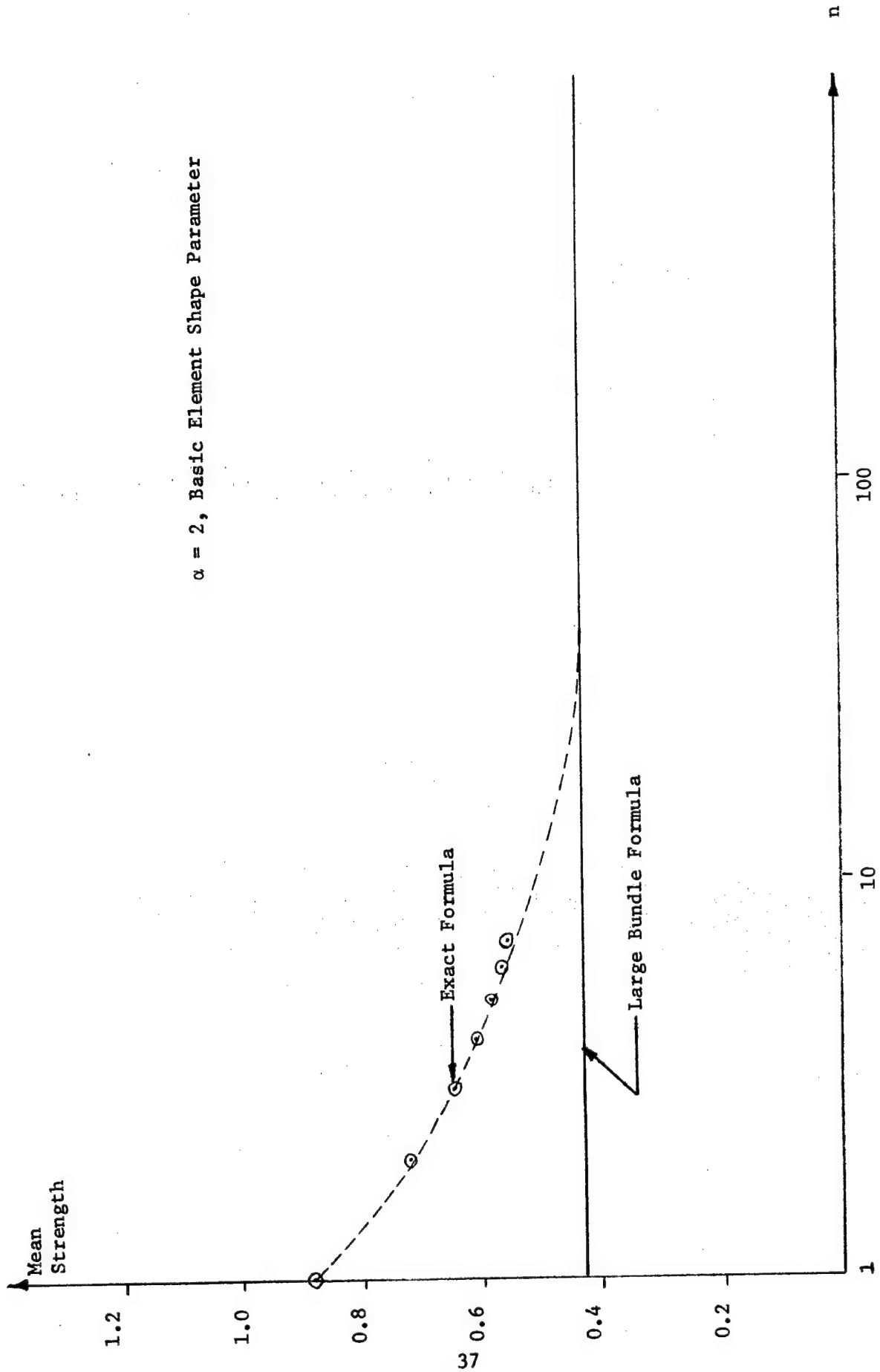$\beta =$ Basic Element Scale Parameter

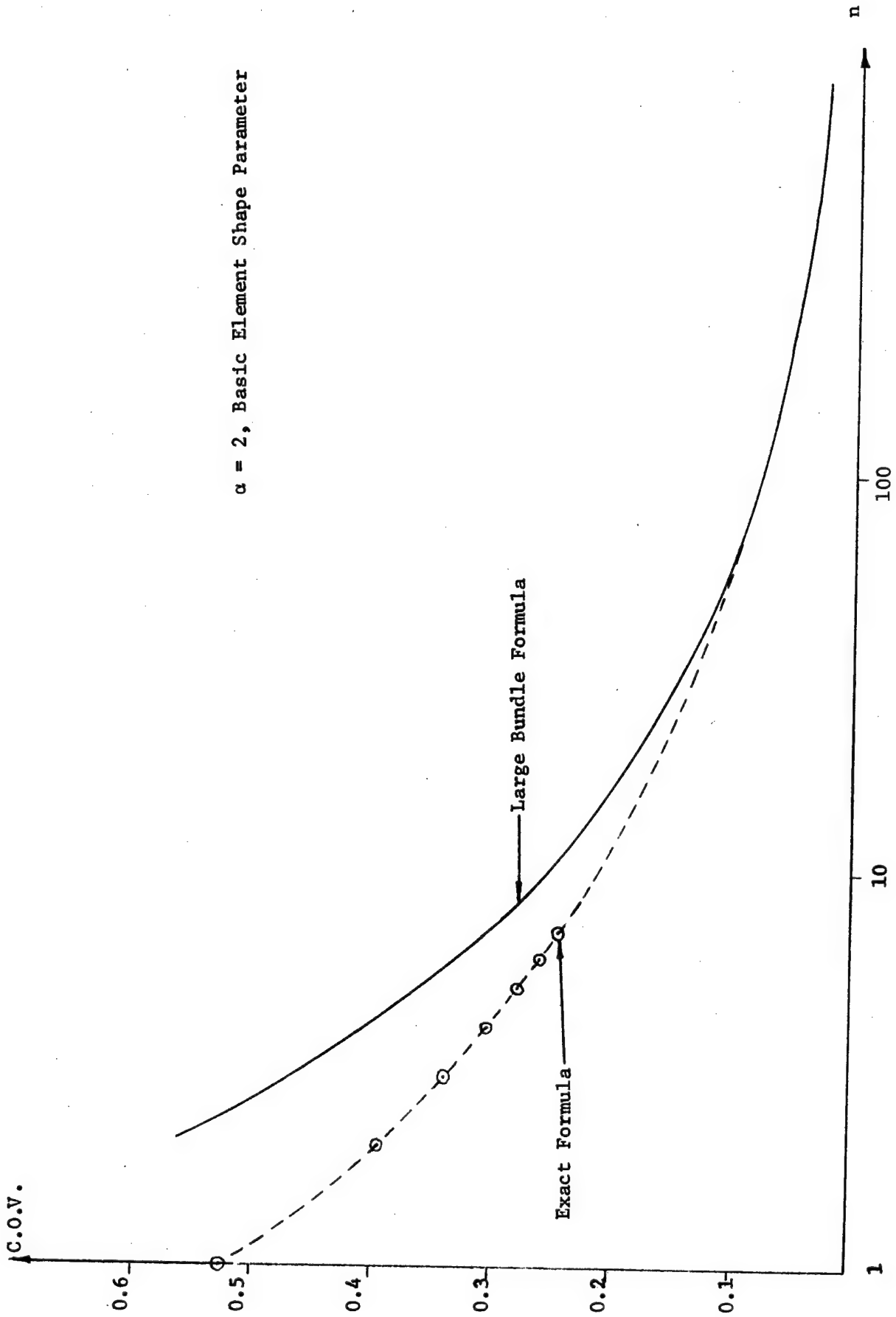36

Figure A-4   Mean Strength for n Elements in Parallel

Figure A-5 Coeficient of Variation for n Elements in Parallel

The in-parallel model subjected to a fatigue loading is considerably more involved than the static case. This is primarily due to the fact that after some fiber failures, the loading in the remaining fibers increases, and the corresponding life distribution also changes. Further analytical work must be done before an expression to predict fatigue life can be presented. The experimental portion of this phase presents some special problems. One problem is the transient loading following a fiber failure may cause additional failures. Another problem is that the load in the surviving fibers, for n=3 or 4, may exceed the static strength. One testing procedure which may prove successful is to operate in the constant stroke mode. The minimum applied load will be 10% of the maximum. The three elements will be placed side by side in the gripping anti-buckling apparatus. When one specimen fails the test will be stopped and the remaining specimens rearranged so as to insure uniform loading. The test will then be restarted and run until the next specimen fails. After positioning the last element the test will proceed to total failure. The total life of the three-in-parallel arrangement will be recorded.

Expanded Formulas for Small Values of n

Eq. (A-2) has been expanded for values of n up to 7. On the following pages these expansions are given. Following these is the computer program listing used to evaluate $P(X^{(n)} \leq x)$, $\mu^{(n)}$ and $\sigma^{(n)}$.

$$\text{Expansion} \quad \text{of} \quad \text{Eq.} \, (A\text{-}2)$$

$$\text{for} \quad n = 3$$

$$P(X^{(3)} \leq x) = (P_1)^3 + 6(P_1)(P_2)(P_3) - 3(P_1)(P_2)^2 - 3(P_1)^2(P_3)$$

$$P_1 = P(X \leq x) = 1 - \exp\left[-(x/\beta)^{\alpha}\right]$$

$$P_2 = P(X \leq \tfrac{3x}{2}) = 1 - \exp\left[-\left(\tfrac{3x}{2\beta}\right)^{\alpha}\right]$$

$$P_3 = P(X \leq 3x) = 1 - \exp\left[-(3x/\beta)^{\alpha}\right]$$

2

Expansion of Eq. $(A-2)$

for $n = 4$

$$P(X^{(4)} \leq x) = -(P1)^4 + 4(P4)(P1)^3 + 4(P2)^3(P1)$$

$$+ 6(P3)^2(P1)^2 - 12(P4)(P3)(P1)^2 - 12(P4)(P2)^2(P1)$$

$$- 12(P3)^2(P2)(P1) + 24(P4)(P3)(P2)(P1)$$

$$P1 = P(X \leq x) = 1 - \exp\left[-(x/\beta)^\alpha\right]$$

$$P2 = P(X \leq \tfrac{4x}{3}) = 1 - \exp\left[-(\tfrac{4x}{3\beta})^\alpha\right]$$

$$P3 = P(X \leq \tfrac{4x}{2}) = 1 - \exp\left[-(\tfrac{4x}{2\beta})^\alpha\right]$$

$$P4 = P(X \leq 4x) = 1 - \exp\left[-(\tfrac{4x}{\beta})^\alpha\right]$$

$$\text{Expansion of Eq. (A-2)}$$
$$\text{for } n = 5$$

$$P(X^{(5)} \leq x) = (P1)^5 - 5(P5)(P1)^4 - 5(P2)^4(P1) - 10(P4)^2(P1)^3$$

$$- 10(P3)^3(P1)^2 + 20(P5)(P4)(P1)^3 + 20(P5)(P2)^3(P1)$$

$$+ 20(P3)^3(P2)(P1) + 30(P4)^2(P2)^2(P1) + 30(P4)^2(P3)(P1)^2$$

$$+ 30(P5)(P3)^2(P1)^2 - 60(P5)(P4)(P3)(P1)^2$$

$$- 60(P5)(P4)(P2)^2(P1) - 60(P5)(P3)^2(P2)(P1)$$

$$- 60(P4)^2(P3)(P2)(P1) + 120(P5)(P4)(P3)(P2)(P1)$$

$$P1 = P(X \leq x) = 1 - \exp\left[-(x/\beta)^\alpha\right]$$

$$P2 = P(X \leq \tfrac{5x}{4}) = 1 - \exp\left[-\left(\tfrac{5x}{4\beta}\right)^\alpha\right]$$

$$P3 = P(X \leq \tfrac{5x}{3}) = 1 - \exp\left[-\left(\tfrac{5x}{3\beta}\right)^\alpha\right]$$

$$P4 = P(X \leq \tfrac{5x}{2}) = 1 - \exp\left[-\left(\tfrac{5x}{2\beta}\right)^\alpha\right]$$

$$P5 = P(X \leq 5x) = 1 - \exp\left[-\left(\tfrac{5x}{\beta}\right)^\alpha\right]$$

$$\text{Expansion} \quad \text{of} \quad Eq. (A\text{-}2)$$
$$\text{for} \quad n = 6$$

$$P(X^{(6)} \leq x) = -(P1)^6 + 6(P6)(P1)^5 + 6(P2)^5(P1) + 15(P5)^2(P1)^4$$

$$+ 15(P3)^4(P1)^2 + 20(P4)^3(P1)^3$$

$$- 30(P6)(P5)(P1)^4 - 30(P6)(P2)^4(P1) - 30(P3)^4(P2)(P1)$$

$$- 60(P5)^2(P4)(P1)^3 - 60(P6)(P4)^2(P1)^3 - 60(P5)^2(P2)^3(P1)$$

$$- 60(P6)(P3)^3(P1)^2 - 60(P4)^3(P3)(P1)^2 - 60(P4)^3(P2)^2(P1)$$

$$+ 120(P6)(P5)(P4)(P1)^3 + 120(P6)(P5)(P2)^3(P1) + 120(P6)(P3)^3(P2)(P1)$$

$$+ 120(P4)^3(P3)(P2)(P1) + 180(P5)^2(P4)(P3)(P1)^2 + 180(P5)^2(P4)(P2)^2(P1)$$

$$+ 180(P5)^2(P3)^2(P2)(P1) + 180(P6)(P5)(P3)^2(P1)^2$$

$$+ 180(P6)(P4)^2(P2)^2(P1) + 180(P6)(P4)^2(P3)(P1)^2$$

$$- 360(P6)(P5)(P4)(P3)(P1)^2 - 360(P6)(P5)(P4)(P2)^2(P1)$$

$$- 360(P6)(P5)(P3)^2(P2)(P1) - 360(P6)(P4)^2(P3)(P2)(P1)$$

$$- 360(P5)^2(P4)(P3)(P2)(P1)$$

$$+ 720(P6)(P5)(P4)(P3)(P2)(P1)$$

$$- 90(P5)^2(P3)^2(P1)^2$$

$$P1 = P(X \leq x) = 1 - \exp\left[-\left(\frac{x}{\beta}\right)^{\alpha}\right]$$

$$P2 = P\left(X \leq \frac{6x}{5}\right) = 1 - \exp\left[-\left(\frac{6x}{5\beta}\right)^{\alpha}\right]$$

$$P3 = P\left(X \leq \frac{6x}{4}\right) = 1 - \exp\left[-\left(\frac{6x}{4\beta}\right)^{\alpha}\right]$$

$$P4 = P\left(X \leq \frac{6x}{3}\right) = 1 - \exp\left[-\left(\frac{6x}{3\beta}\right)^{\alpha}\right]$$

$$P5 = P\left(X \leq \frac{6x}{2}\right) = 1 - \exp\left[-\left(\frac{6x}{2\beta}\right)^{\alpha}\right]$$

$$P6 = P(X \leq 6x) = 1 - \exp\left[-\left(\frac{6x}{\beta}\right)^{\alpha}\right]$$

2

Expansion of Eq. (A-2)

for $n = 7$

$$P(X^{(7)} \leq x) = (P1)^7 - 7(P7)(P1)^6 - 7(P2)^6(P1) - 21(P6)^2(P1)^5$$

$$- 21(P3)^5(P1)^2 - 35(P5)^3(P1)^4 - 35(P4)^4(P1)^3$$

$$+ 42(P7)(P6)(P1)^5 + 42(P7)(P2)^5(P1) + 42(P3)^5(P2)(P1)$$

$$+ 105(P6)^2(P5)(P1)^4 + 105(P7)(P5)^2(P1)^4 + 105(P6)^2(P2)^4(P1)$$

$$+ 105(P7)(P3)^4(P1)^2 + 105(P4)^4(P2)^2(P1) + 105(P4)^4(P3)(P1)$$

$$+ 210(P6)^2(P4)^2(P1)^3 + 210(P6)^2(P3)^3(P1)^2 + 210(P5)^3(P3)^2(P1)^2$$

$$+ 140(P5)^3(P2)^3(P1) + 140(P5)^3(P4)(P1)^3 + 140(P7)(P4)^3(P1)^3$$

$$- 210(P7)(P6)(P5)(P1)^4 - 210(P7)(P6)(P2)^4(P1)$$

$$- 210(P7)(P3)^4(P2)(P1) - 210(P4)^4(P3)(P2)(P1)$$

$$- 420(P7)(P6)(P4)^2(P1)^3 - 420(P7)(P6)(P3)^3(P1)^2$$

$$- 420(P7)(P5)^2(P4)(P1)^3 - 420(P6)^2(P5)(P4)(P1)^3$$

$$- 420(P5)^3(P4)(P2)^2(P1) - 420(P7)(P4)^3(P2)^2(P1)$$

$$- 420(P7)(P5)^2(P2)^3(P1) - 420(P5)^3(P3)^2(P2)(P1)$$

$$-420(P6)^2(P3)^2(P2)(P1) - 420(P7)(P4)^3(P3)(P1)^2$$

$$-420(P5)^3(P4)(P3)(P1)^2 - 420(P6)^2(P5)(P2)^3(P1)$$

$$-630(P7)(P5)^2(P3)^2(P1)^2 - 630(P6)^2(P5)(P3)^2(P1)^2$$

$$-630(P6)^2(P4)^2(P3)(P1)^2 - 630(P6)^2(P4)^2(P2)^2(P1)$$

$$+840(P7)(P6)(P5)(P4)(P1)^3 + 840(P7)(P6)(P5)(P2)^3(P1)$$

$$+840(P7)(P6)(P3)^3(P2)(P1) + 840(P7)(P4)^3(P3)(P2)(P1)$$

$$+840(P5)^3(P4)(P3)(P2)(P1)$$

$$+1260(P7)(P6)(P5)(P3)^2(P1)^2 + 1260(P7)(P6)(P4)^2(P3)(P1)^2$$

$$+1260(P7)(P5)^2(P4)(P3)(P1)^2 + 1260(P6)^2(P5)(P4)(P3)(P1)^2$$

$$+1260(P6)^2(P5)(P4)(P2)^2(P1) + 1260(P7)(P5)^2(P4)(P2)^2(P1)$$

$$+1260(P7)(P6)(P4)^2(P2)^2(P1) + 1260(P6)^2(P4)^2(P3)(P2)(P1)$$

$$+1260(P7)(P5)^2(P3)^2(P2)(P1) + 1260(P6)^2(P5)(P3)^2(P2)(P1)$$

$$-2520(P7)(P6)(P5)(P4)(P3)(P1)^2 - 2520(P7)(P6)(P5)(P4)(P2)^2(P1)$$

$$-2520(P7)(P6)(P5)(P3)^2(P2)(P1) - 2520(P7)(P6)(P4)^2(P3)(P2)(P1)$$

$$-2520(P7)(P5)^2(P4)(P3)(P2)(P1) - 2520(P6)^2(P5)(P4)(P3)(P2)(P1)$$

$$+5040(P7)(P6)(P5)(P4)(P3)(P2)(P1)$$

$$P1 = P(X \leq x) = 1 - \exp\left[-\left(\frac{x}{\beta}\right)^{\alpha}\right]$$

$$P2 = P\left(X \leq \frac{7x}{6}\right) = 1 - \exp\left[-\left(\frac{7x}{6\beta}\right)^{\alpha}\right]$$

$$P3 = P\left(X \leq \frac{7x}{5}\right) = 1 - \exp\left[-\left(\frac{7x}{5\beta}\right)^{\alpha}\right]$$

$$P4 = P\left(X \leq \frac{7x}{4}\right) = 1 - \exp\left[-\left(\frac{7x}{4\beta}\right)^{\alpha}\right]$$

$$P5 = P\left(X \leq \frac{7x}{3}\right) = 1 - \exp\left[-\left(\frac{7x}{3\beta}\right)^{\alpha}\right]$$

$$P6 = P\left(X \leq \frac{7x}{2}\right) = 1 - \exp\left[-\left(\frac{7x}{2\beta}\right)^{\alpha}\right]$$

$$P7 = P(X \leq 7x) = 1 - \exp\left[-\left(\frac{7x}{\beta}\right)^{\alpha}\right]$$

2

Computer Listing for $P(X^{(n)} \leq x)$, $\mu^{(n)}$ and $\sigma^{(n)}$

```
                                                      OPROPA /MF2336
                                                      ================

                                                      START OF SEGMENT
        DIMENSION Q(300),Y(300),U(300),V(300),UU(300),VV(300),
       1VAN(300)
        NP=501
        B=24.
        DO 88 N=1,NP
```

Fortran for expansion of Eq. (A-2) for n = 2, 3, 4, 5, 6, 7 is given on the following pages and is to be inserted in this location of program.

```
88      CONTINUE
50      I=1
51      CONTINUE
        IF(I.LT.3)GO TO 1000
        IF(I.GT.NP)GO TO 2000
        IF(I.GT.NP-5)GO TO 1500
        X1=Q(I-2)
        X2=Q(I-1)
        X3=Q(I)
        X4=Q(I+1)
        X5=Q(I+2)
        X6=Q(I+3)
        Y1=Y(I-2)
        Y2=Y(I-1)
        Y3=Y(I)
        Y4=Y(I+1)
        Y5=Y(I+2)
        Y6=Y(I+3)
69      X=X3
        YA=Y3
70      IF(I.EQ.NP-3)GO TO 2000
100     TERM1=((X-X2)*(X-X4)*(X-X5)*(X-X6)*Y1)/((X1-X2)*(X1-X3)*(X1-X4)*(
       1X1-X5)*(X1-X6))
110     TERM2=((X-X1)*(X-X4)*(X-X5)*(X-X6)*Y2)/((X2-X1)*(X2-X3)*(X2-X4)*(X
       12-X5)*(X2-X6))
120     DEN3=(X3-X1)*(X3-X2)*(X3-X4)*(X3-X5)*(X3-X6)
121     TERM3A=(X-X2)*(X-X4)*(X-X5)*(X-X6)*Y3/DEN3
122     TERM3B=(X-X1)*(X-X4)*(X-X5)*(X-X6)*Y3/DEN3
123     TERM3C=(X-X1)*(X-X2)*(X-X5)*(X-X6)*Y3/DEN3
124     TERM3D=(X-X1)*(X-X2)*(X-X4)*(X-X6)*Y3/DEN3
125     TERM3E=(X-X1)*(X-X2)*(X-X4)*(X-X5)*Y3/DEN3
127     TERM3=TERM3A+TERM3B+TERM3C+TERM3D+TERM3E
```

```
130   TERM4=((X-X1)*(X-X2)*(X-X5)*(X-X6)*Y4)/((X4-X1)*(X4-X2)*(X4-X3)*(X
      14-X5)*(X4-X6))
140   TERM5=((X-X1)*(X-X2)*(X-X4)*(X-X6)*Y5)/((X5-X1)*(X5-X2)*(X5-X3)*(X
      15-X4)*(X5-X6))
150   TERM6=((X-X1)*(X-X2)*(X-X4)*(X-X5)*Y6)/((X6-X1)*(X6-X2)*(X6-X3)*(X
      16-X4)*(X6-X5))
155   CONTINUE
160   DERT=TERM1+TERM2+TERM3+TERM4+TERM5+TERM6
      XDERT=X*DERT
170   PRINT 180,X,YA,DERT,XDERT
180   FORMAT(1H ,"X=",E15.8,10X,"Y=",F15.8,10X,"DY/DX=",F15.8,10X,"XDERT
      1=",E15.8)
      U(I)=X
      VAN(I)=DERT
      V(I)=XDERT
185   FORMAT(F15.8,E15.8)
190   I=I+1
200   GO TO 51
1000  CONTINUE
      X1=O(I)
      X2=O(I+1)
      X3=O(I+2)
      X4=O(I+3)
      X5=O(I+4)
      X6=O(I+5)
      Y1=Y(I)
      Y2=Y(I+1)
      Y3=Y(I+2)
      Y4=Y(I+3)
      Y5=Y(I+4)
      Y6=Y(I+5)
      X=X1
      YA=Y1
      DEN1=(X1-X2)*(X1-X3)*(X1-X4)*(X1-X5)*(X1-X6)
      DEN2=(X2-X1)*(X2-X3)*(X2-X4)*(X2-X5)*(X2-X6)
      DEN3=(X3-X1)*(X3-X2)*(X3-X4)*(X3-X5)*(X3-X6)
      DEN4=(X4-X1)*(X4-X2)*(X4-X3)*(X4-X5)*(X4-X6)
      DEN5=(X5-X1)*(X5-X2)*(X5-X3)*(X5-X4)*(X5-X6)
      DEN6=(X6-X1)*(X6-X2)*(X6-X3)*(X6-X4)*(X6-X5)
      TERM1A=(X-X3)*(X-X4)*(X-X5)*(X-X6)*Y1/DEN1
      TERM1B=(X-X2)*(X-X4)*(X-X5)*(X-X6)*Y1/DEN1
      TERM1C=(X-X2)*(X-X3)*(X-X5)*(X-X6)*Y1/DEN1
      TERM1D=(X-X2)*(X-X3)*(X-X4)*(X-X6)*Y1/DEN1
      TERM1E=(X-X2)*(X-X3)*(X-X4)*(X-X5)*Y1/DEN1
      TERM1=TERM1A+TERM1B+TERM1C+TERM1D+TERM1E
      TERM2=(X-X3)*(X-X4)*(X-X5)*(X-X6)*Y2/DEN2
      TERM3=(X-X2)*(X-X4)*(X-X5)*(X-X6)*Y3/DEN3
      TERM4=(X-X2)*(X-X3)*(X-X5)*(X-X6)*Y4/DEN4
      TERM5=(X-X2)*(X-X3)*(X-X4)*(X-X6)*Y5/DEN5
      TERM6=(X-X2)*(X-X3)*(X-X4)*(X-X5)*Y6/DEN6
      GO TO 155
1500  CONTINUE
1510  CONTINUE
      X1=O(I-5)
      X2=O(I-4)
      X3=O(I-3)
      X4=O(I-2)
      X5=O(I-1)
      X6=O(I)
      Y1=Y(I-5)
      Y2=Y(I-4)
      Y3=Y(I-3)
      Y4=Y(I-2)
```

```
          Y5=Y(I-1)
          Y6=Y(I)
          X=X6
          YA=Y6
          DEN1=(X1-X2)*(X1-X3)*(X1-X4)*(X1-X5)*(X1-Y6)
          DEN2=(X2-X1)*(X2-X3)*(X2-X4)*(X2-X5)*(X2-Y6)
          DEN3=(X3-X1)*(X3-X2)*(X3-X4)*(X3-X5)*(X3-Y6)
          DEN4=(X4-X1)*(X4-X2)*(X4-X3)*(X4-X5)*(X4-X6)
          DEN5=(X5-X1)*(X5-X2)*(X5-X3)*(X5-X4)*(X5-X6)
          DEN6=(X6-X1)*(Y6-X2)*(X6-X3)*(Y6-X4)*(X6-X5)
          TERM1=(X-X2)*(X-X3)*(X-X4)*(X-X5)*Y1/DEN1
          TERM2=(X-X1)*(X-X3)*(X-X4)*(X-X5)*Y2/DEN2
          TERM3=(X-X1)*(X-X2)*(X-X4)*(X-X5)*Y3/DEN3
          TERM4=(X-X1)*(X-X2)*(X-X3)*(X-X5)*Y4/DEN4
          TERM5=(X-X1)*(X-X2)*(X-X3)*(X-X4)*Y5/DEN5
          TERM6A=(Y-Y2)*(X-X3)*(X-X4)*(X-X5)*Y6/DEN6
          TERM6B=(X-X1)*(X-X3)*(X-X4)*(X-X5)*Y6/DEN6
          TERM6C=(X-X1)*(X-X2)*(X-X4)*(X-X5)*Y6/DEN6
          TERM6D=(X-X1)*(X-X2)*(X-X3)*(X-X5)*Y6/DEN6
          TERM6E=(X-X1)*(X-X3)*(X-X2)*(Y-X4)*Y6/DEN6
          TERM6=TERM6A+TERM6B+TERM6C+TERM6D+TERM6E
          DERT=TERM1+TERM2+TERM3+TERM4+TERM5+TERM6
          XDERT=X*DERT
          PRINT 150,X,YA,DERT,XDERT
          U(I)=X
          VAN(I)=DERT
          V(I)=XDERT
          I=I+I
          IF(I.GT.NP) GO TO 2000
          GO TO 1510
   2000   CONTINUE
          IDENT=0
   7009   CONTINUE
          AREA=0.
          NPM1=NP-1
          DO 30 I=1,NPM1
          UU(I)=U(I+1)
          VV(I)=V(I+1)
          XINC=UU(I)-U(I)
          YMID=(       V(I)+VV(I))/2.
          ADDEND=XINC*YMID
          AREA=ADDEND+AREA
          PRINT25,U(I),V(I),ADDEND,AREA
   25     FORMAT(1H ,"X=",E15.8,10X,"Y=",F15.8,10X,"ADDEND=",F15.8,10X,
         1"AREA=",F15.8)
   30     CONTINUE
          PRINT 40,AREA
   40     FORMAT(///,1H ,"THE TOTAL AREA =",E15.8)
          IF(IDENT.GT.0) GO TO 7021
          XMU=AREA
          DO 7001 I=1,NP
          V(I)=(U(I)-XMU)**2*VAN(I)
   7001   CONTINUE
          IDENT=1
          GO TO 7009
   7021   SIGMA=SQRT(AREA)
          CV=SIGMA/XMU
          PRINT 7042,XMU,SIGMA,CV
   7042   FORMAT(1H ,"XMU=",E15.8," SIGMA=",E15.8," CV=",E15.8)
          CALL EXIT
          END
```
SEGMENT

50

Fortran for In-Parallel Model, n = 2

```
      ARG1=.01*(N -1)
      ARG2=2.*ARG1
      P1=1.-EXP(-ARG1**B)
      P2=1.-EXP(-ARG2**B)
      PTW=2.*P1*P2-P1**2
      Q(N)=ARG1
      Y(N)=PTW
      PRINT 89,ARG1,P1,PTW
   89 FORMAT(1H ,"ARG1=",E15.8," P1=",E15.8," PTW=",E15.8)
```

Fortran for In-Parallel Model, n = 3

```
      ARG1=.01*(N -1)
      ARG2=1.5*ARG1
      ARG3=3.0*ARG1
      P1=1.-EXP(-ARG1**B)
      P2=1.-EXP(-ARG2**B)
      P3=1.-EXP(-ARG3**B)
      PTH=P1**3+6.*P1*P2*P3-3.*P1*P2**2-3.*P1**2*P3
      Q(N)=ARG1
      Y(N)=PTH
      PRINT 89,ARG1,P1,PTH
   89 FORMAT(1H ,"ARG1=",E15.8," P1=",E15.8," PTH=",E15.8)
```

Fortran for In-Parallel Model, n = 4

```
      ARG1=.01*(N -1)
      ARG3=2.*ARG1
      ARG2=4.*ARG1/3.
      ARG4=4.*ARG1
      P1=1.-EXP(-ARG1**B)
      P2=1.-EXP(-ARG2**B)
      P3=1.-EXP(-ARG3**B)
      P4=1.-EXP(-ARG4**B)
      PFR=24.*P4*P3*P2*P1-12.*P3**2*P2*P1-12.*P4*P2**2*P1-
     1 12.*P4*P3*P1**2+4.*P2**3*P1+6.*P3**2*P1**2+4.*P4*P1**3-P1**4
      Q(N)=ARG1
      Y(N)=PFR
      PRINT 89,ARG1,P1,PFR
   89 FORMAT(1H ,"ARG1=",F15.8," P1=",E15.8," PFR=",E15.8)
```

Fortran for In-Parallel Model, n = 5

```
          ARG1=.01*(N -1)
          ARG2=5.*ARG1/4.
          ARG3=5.*ARG1/3.
          ARG4=5.*ARG1/2.
          ARG5=5.*ARG1
          P1=1.-EXP(-ARG1**B)
          P2=1.-EXP(-ARG2**B)
          P3=1.-EXP(-ARG3**B)
          P4=1.-EXP(-ARG4**B)
          P5=1.-EXP(-ARG5**B)
          PFV=P1**5-5.*P5*P1**4-5.*P2**4*P1-10.*P4**2*P1**3
     1   -10.*P3**3*P1**2
     2   +20.*P5*P4*P1**3+20.*P5*P2**3*P1+20.*P3**3*P2*P1
     3   +30.*P4**2*P2**2*P1+30.*P4**2*P3*P1**2+30.*P5*P3**2*P1**2
     4   -60.*P5*P4*P3*P1**2-60.*P5*P4*P2**2*P1-60.*P5*P3**2*P2*P1
     5   -60.*P4**2*P3*P2*P1+120.*P1*P2*P3*P4*P5
          G(N)=ARG1
          Y(N)=PFV
          PRINT 89,ARG1,P1,PFV
     89   FORMAT(1H ,"ARG1=",F15.8," P1=",F15.8," PFV=",E15.8)
```

Fortran for In-Parallel Model, n = 6

```
          ARG1=.01*(N -1)
          ARG2=6.*ARG1/5.
          ARG3=6.*ARG1/4.
          ARG4=6.*ARG1/3.
          ARG5=6.*ARG1/2.
          ARG6=6.*ARG1
          P1=1.-EXP(-ARG1**B)
          P2=1.-EXP(-ARG2**B)
          P3=1.-EXP(-ARG3**B)
          P4=1.-EXP(-ARG4**B)
          P5=1.-EXP(-ARG5**B)
          P6=1.-EXP(-ARG6**B)
          PSX=-P1**6+6.*P6*P1**5+6.*P2**5*P1+15.*P5**2*P1**4
     1   +15.*P3**4*P1**2+20.*P4**3*P1**3
     2   -30.*P6*P5*P1**4-30.*P6*P2**4*P1-30.*P3**4*P2*P1
     3   -60.*P5**2*P4*P1**3-60.*P6*P4**2*P1**3-60.*P5**2*P2**3*P1
     4   -60.*P6*P3**3*P1**2-60.*P4**3*P3*P1**2-60.*P4**3*P2**2*P1
     5   +120.*P6*P5*P4*P1**3+120.*P6*P5*P2**3*P1
     *   +120.*P6*P3**3*P2*P1
     6   +120.*P4**3*P3*P2*P1+180.*P5**2*P4*P3*P1**2+180.*P5**2*P4*P2**2*P1
     7   +180.*P5**2*P3**2*P2*P1+180.*P6*P5*P3**2*P1**2
     8   +180.*P6*P4**2*P2**2*P1
     9   +180.*P6*P4**2*P3*P1**2
     *   -360.*P6*P5*P4*P3*P1**2-360.*P6*P5*P4*P2**2*P1
     *   -360.*P6*P5*P3**2*P2*P1-360.*P6*P4**2*P3*P2*P1
     *   -360.*P5**2*P4*P3*P2*P1
     *   +720.*P6*P5*P4*P3*P2*P1
     *   -90.*P5**2*P3**2*P1**2
          Q(N)=ARG1
          Y(N)=PSX
          PRINT 89,ARG1,P1,PSX
     89   FORMAT(1H ,"ARG1=",E15.8," P1=",E15.8," PSX=",E15.8)
```

Fortran for In-Parallel Model, n = 7

```
        ARG1=.01*(N -1)
        ARG2=7.*ARG1/6.
        ARG3=7.*ARG1/5.
        ARG4=7.*ARG1/4.
        ARG5=7.*ARG1/3.
        ARG6=7.*ARG1/2.
        ARG7=7.*ARG1
        P1=1.-EXP(-ARG1**B)
        P2=1.-EXP(-ARG2**B)
        P3=1.-EXP(-ARG3**B)
        P4=1.-EXP(-ARG4**B)
        P5=1.-EXP(-ARG5**B)
        P6=1.-EXP(-ARG6**B)
        P7=1.-EXP(-ARG7**B)
        PSV=P1**7-7.*P7*P1**6-7.*P2**6*P1
       *-21.*P6**2*P1**5-21.*P3**5*P1**2-35.*P5**3*P1**4
       *-35.*P4**4*P1**3
       *+42.*P7*P6*P1**5+42.*P7*P2**5*P1+42.*P3**5*P2*P1
       *+105.*P6**2*P5*P1**4+105.*P7*P5**2*P1**4+105.*P6**2*P2**4*P1
       *+105.*P7*P3**4*P1**2+105.*P4**4*P2**2*P1
       *+105.*P4**4*P3*P1**2
       *+210.*P6**2*P4**2*P1**3+210.*P6**2*P3**3*P1**2
       *+210.*P5**3*P3**2*P1**2
       *+140.*P5**3*P2**3*P1+140.*P5**3*P4*P1**3
       *+140.*P7*P4**3*P1**3
       *-210.*P7*P6*P5*P1**4-210.*P7*P6*P2**4*P1
       *-210.*P7*P3**4*P2*P1-210.*P4**4*P3*P2*P1
       *-420.*P7*P6*P4**2*P1**3-420.*P7*P6*P3**3*P1**2
       *-420.*P7*P5**2*P4*P1**3-420.*P6**2*P5*P4*P1**3
       *-420.*P5**3*P4*P2**2*P1-420.*P7*P4**3*P2**2*P1
       *-420.*P7*P5**2*P2**3*P1-420.*P5**3*P3**2*P2*P1
       *-420.*P6**2*P3**3*P2*P1-420.*P7*P4**3*P3*P1**2
       *-420.*P5**3*P4*P3*P1**2-420.*P6**2*P5*P2**3*P1
       *-630.*P7*P5**2*P3**2*P1**2-630.*P6**2*P5*P3**2*P1**2
       *-630.*P6**2*P4**2*P3*P1**2-630.*P6**2*P4**2*P2**2*P1
       *+840.*P7*P6*P5*P4*P1**3+840.*P7*P6*P5*P2**3*P1
       *+840.*P7*P6*P3**3*P2*P1+840.*P7*P4**3*P3*P2*P1
       *+840.*P5**3*P4*P3*P2*P1
       *+1260.*P7*P6*P5*P3**2*P1**2+1260.*P7*P6*P4**2*P3*P1**2
       *+1260.*P7*P5**2*P4*P3*P1**2+1260.*P6**2*P5*P4*P3*P1**2
       *+1260.*P6**2*P5*P4*P2**2*P1+1260.*P7*P5**2*P4*P2**2*P1
       *+1260.*P7*P6*P4**2*P2**2*P1+1260.*P6**2*P4**2*P3*P2*P1
       *+1260.*P7*P5**2*P3**2*P2*P1+1260.*P6**2*P5*P3**2*P2*P1
       *-2520.*P7*P6*P5*P4*P3*P1**2-2520.*P7*P6*P5*P4*P2**2*P1
       *-2520.*P7*P6*P5*P3**2*P2*P1-2520.*P7*P6*P4**2*P3*P2*P1
       *-2520.*P7*P5**2*P4*P3*P2*P1-2520.*P6**2*P5*P4*P3*P2*P1
       *+5040.*P7*P6*P5*P4*P3*P2*P1.
        U(N)=ARG1
        Y(N)=PSV
        PRINT 89,ARG1,P1,PSV
89      FORMAT(1H ,"ARG1=",E15.8," P1=",E15.8," PSV=",E15.8)
```
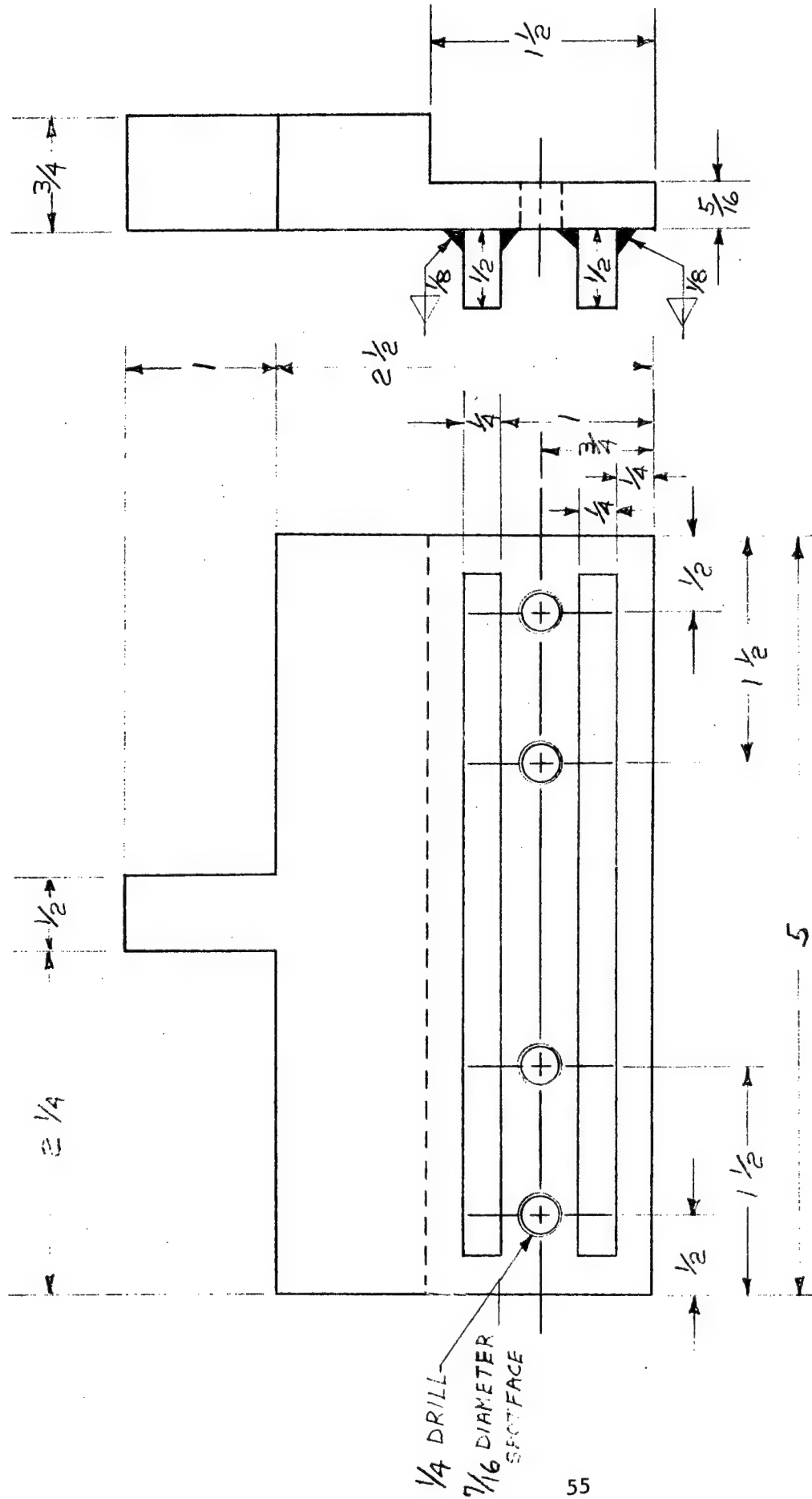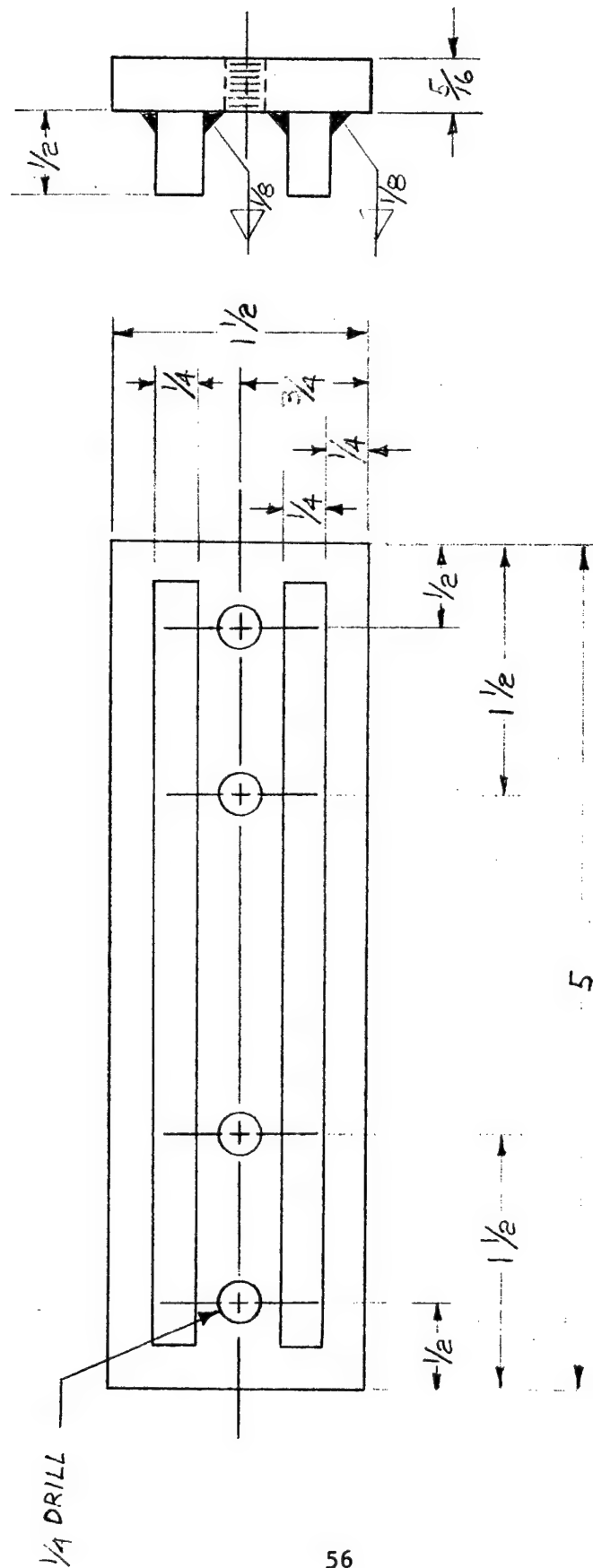
Appendix B   Detail Drawings for Gripping Anti-Buckling Guide Device

Material: Hot Rolled Steel

Figure B-1   Front Grip
(All Dimensions in Inch, 1 = 25.4 mm)

55

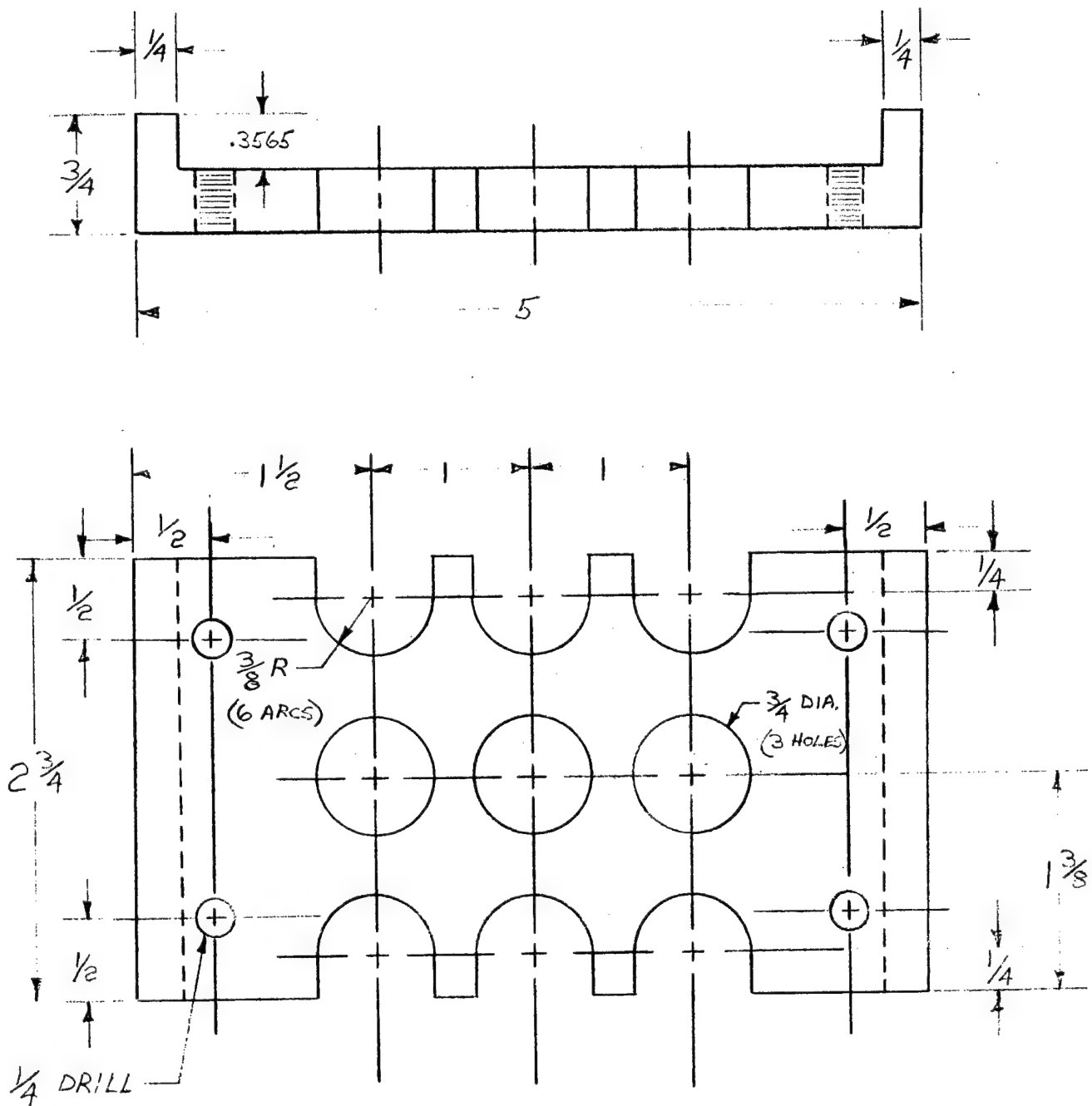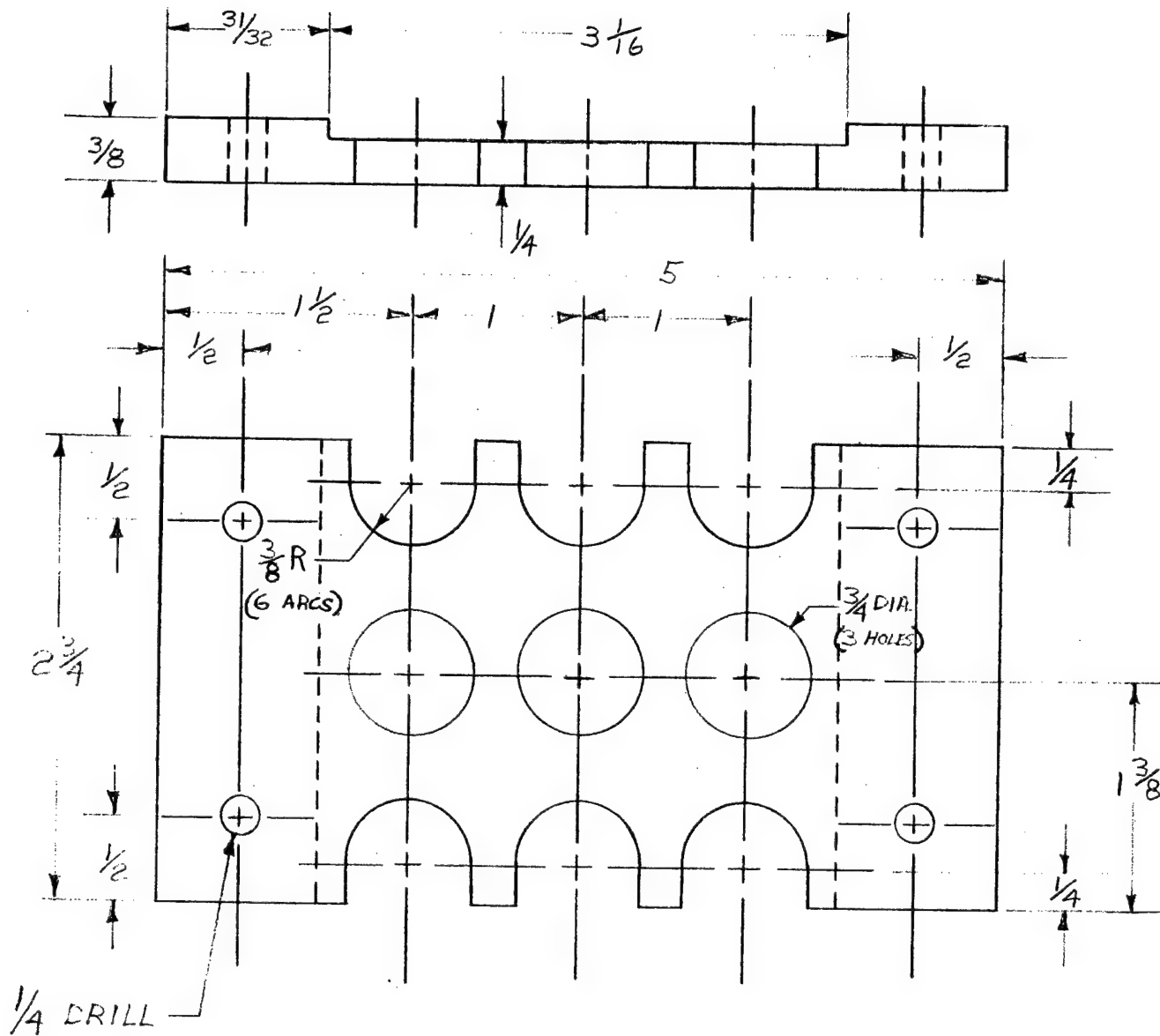Material: Hot Rolled Steel

Figure B-2 Rear-Grip
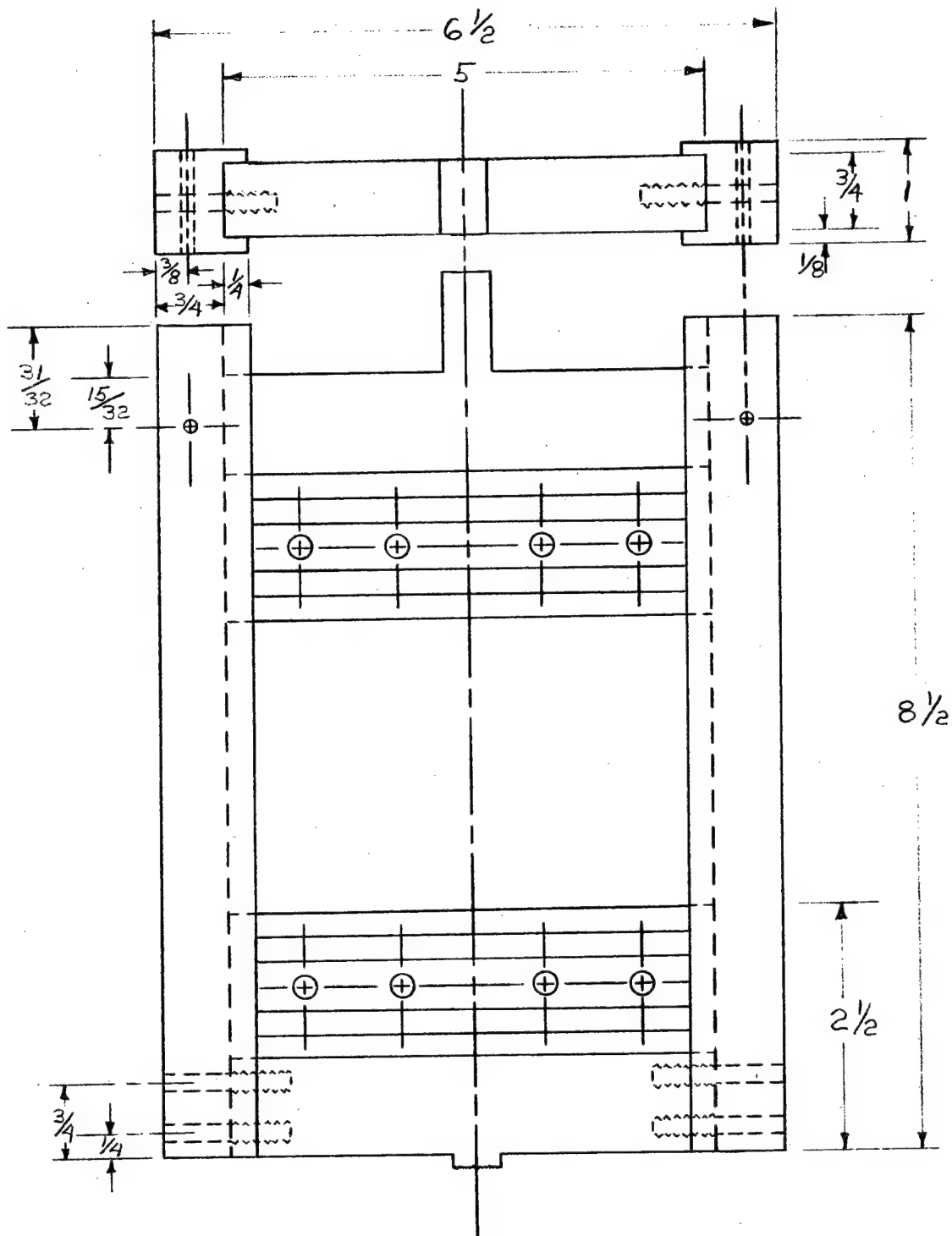(All Dimensions in Inch, 1 in = 25.4 mm)

56

Material: Aluminum

Figure B-3 Front Anti-Buckling Guide
(All Dimensions in Inch, 1 in = 25.4 mm)

Material: Aluminum

Figure B-4   Rear Anti-Buckling Guide
(All Dimensions in Inch, 1 = in = 25.4 mm)

58

Material: Steel

Figure B-5 Sub-Assembly, Runners and Grips
(All Dimensions in Inch, 1 = 25.4 mm)

Appendix C.   Additional Data

Some additional fatigue tests were performed with elements having different geometries. All tests were performed with the same loading conditions as described in the main body of this report. The first set of tests was performed with elements containing four 1/4 inch (6.4 mm) holes as shown in Fig. C-1. Table C-I gives the life and the failure location of these elements. The mean life is 5430 cycles. This is much less than the in-series model prediction life. Due to the fact that all elements failed through the bottom hole it was concluded that its location was too near to the end tab and thus experienced a greater load than the other three.

Several months later a series of fatigue tests were performed on elements containing two 1/4 inch (6.4 mm) holes as shown in Fig. C-2. The initial tests in this series were performed with configuration 1 type elements. These all broke through the bottom hole. The geometry was altered by moving the two holes further apart as shown as configuration 2. These also all broke through the bottom hole and had shorter life than configuration 1 elements. The lives for these two configurations are shown in Table C-II.

In order to see if the position of the hole in an element affected the life, a series of three tests were performed with an element with a 1/4 inch (6.4 mm) hole located near the bottom end tab as seen in Fig. C-3. Table C-III records the life for these tests. As can be seen the lives are much shorter than the lives recorded for the basic element (Table Ia).

Table C-I

Compression Fatigue Life of 4 In-Series Specimen, Graphite/Epoxy $[\pm 45, 0_2, \overline{\pm} 45]_s$

Max. Stress = 74% Basic Element Mean Static Strength $R = -\infty$, Frequency = 5 Hz (5 specimens)

Failure Location	Life (cycles)
Bottom	320
Bottom	3180
Bottom	4480
Bottom	7520
Bottom	11630

$\bar{x} = 5430$
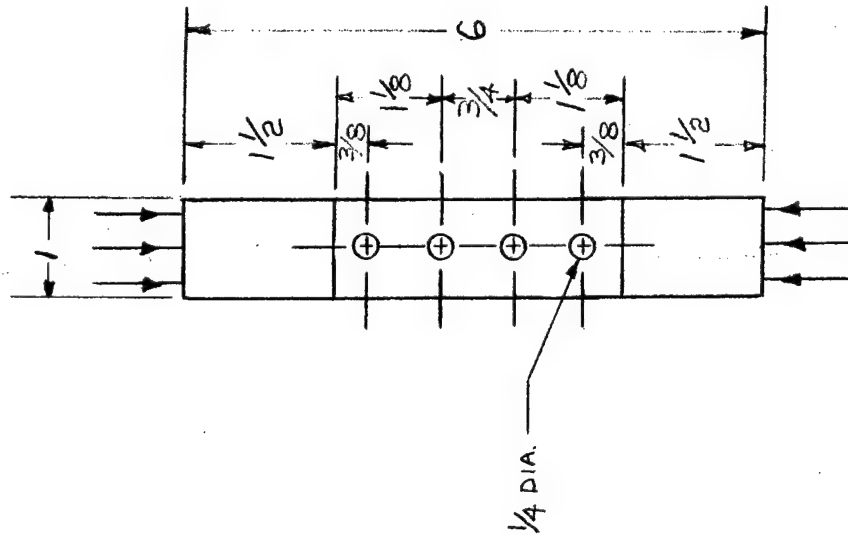
Figure C-1 Four-In-Series Element

(All Dimensions in Inch, 1 in = 25.4 mm)

Table C-II

Compression Fatigue Life of 2 In-Series Specimen, Graphite/Epoxy $[\pm 45, 0_2, \overline{+45}]_s$

Max. Stress = 74% Basic Element Mean Static Strength, R = $-\infty$, Frequency = 5 Hz (7 specimens)

Failure Location	Configuration	Life (cycles)
Bottom	1	140
Bottom	2	1150
Bottom	1	1900
Bottom	2	12700
Bottom	1	53320
Bottom	1	58730
Bottom	1	119290

Configuration 2

Configuration 1
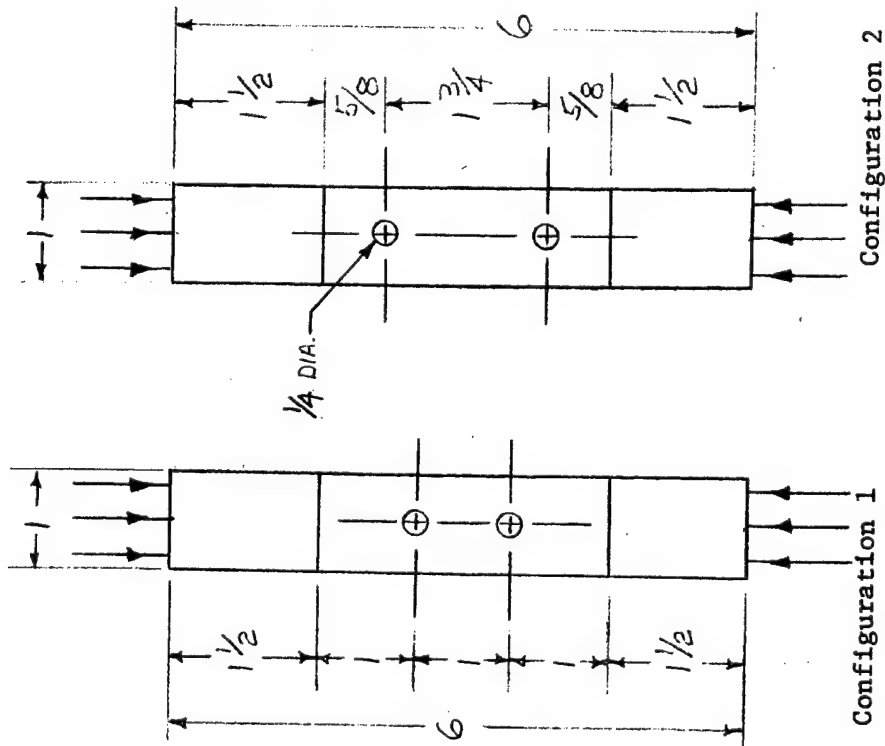
Figure C-2   Two-In-Series Elements

(All Dimensions in Inch, 1 in = 25.4 mm)

62

Table C-III

Compression Fatigue Life of Single Hole Specimen, Graphite/Epoxy $[\pm 45, 0_2, +45]_s$

Max. Compression Load = 74% Basic Element Mean Static Strength, R = -∞, Freq. = 5 Hz (10 specimens).

Failure Location	Life (cycles)
Hole	1*
Hole	1020
Hole	1900

* Broke in loading.
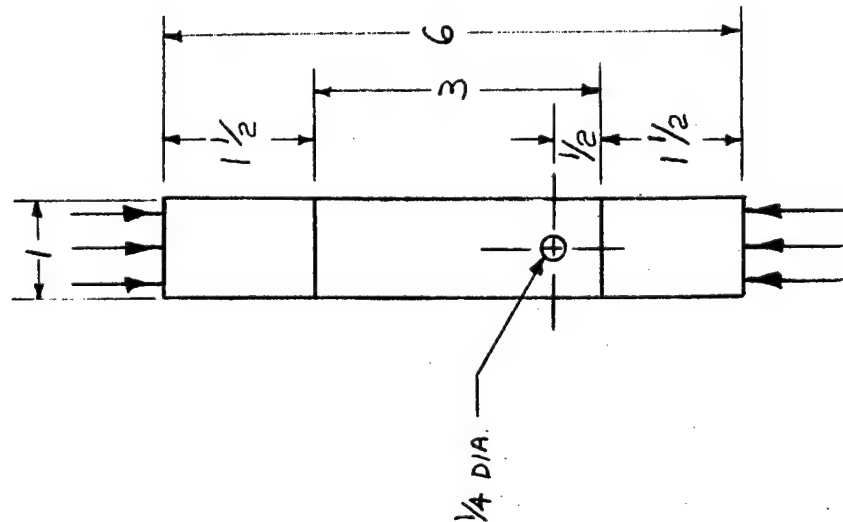
Figure C-3 Single Hole Element

(All Dimensions in Inch, 1 in = 25.4 mm)

This tends to indicate that the closer the hole to the bottom end tab, the greater will be the force seen by the hole and hence the shorter the life.

The results obtained in Tables C-I-III tend to indicate that the stress distribution is not uniform throughout the total length of the specimen. Since the dynamic loading is applied by the accuator to the bottom of the specimen, the stress concentration at the bottom hole is greater than at the other holes.

This evidence is of course not conclusive. Other plausible explanations can be forwarded. First the original basic and three-in-series elements were taken from one end of the plate whereas the elements discussed in this paragraph were obtained from the other end of the plate. It is conceivable that the two ends of the plate had different properties and thus the elements taken from each constituted distinct populations. A randomized scheme of picking test elements of course would have eliminated this possibility. Another explanation was that the tests listed in Tables I, II and Tables C-I-III were performed before and after respectively a major breakdown and repair of the Instron testing machine. Also, the gripping anti-buckling guide may have been inserted in the Instron improperly. In short, due to the uncertainties associated with Tables C-I-III no further analysis was attempted on this data.

DISTRIBUTION LIST

Government Activities

	No. of Copies
NAVAIRSYSCOM, AIR-954 (2 for retention), 2 for AIR-530, 1 for AIR-320B, AIR-52032D, AIR-5302, AIR-53021, AIR-530215).	9
AFFDL, WPAFB, OH 45433	2
(Attn: FB/Mr. P. A. Parmley)	1
(Attn: FBC/Mr. C. Wallace)	1
(Attn: FBC/Mr. E. E. Zink)	1
AFML, WPAFB, OH 45433	
(Attn: LAM (Technical Library)).	1
(Attn: LT-1/Mr. W. R. Johnston).	1
(Attn: LTF/Mr. T. Cordell)	1
(Attn: FBSC/Mr. L. Kelly).	1
(Attn: MAC/Mr. G. P. Peterson)	1
(Attn: MXA/Mr. F. J. Fechek)	1
(Attn: MBC/Mr. T. G. Reinhard, Jr.).	1
AFOSR, Washington, D.C. 20333	1
(Attn: Mr. J. Pomerantz)	
DDC.	12
FAA, Airframes Branch, ES-120, Washington, D.C. 20553	1
(Attn: Mr. J. Dougherty)	
NASA (ADM), Washington, D.C. 20546	1
(Attn: Secretary).	
NASA, George C. Marshall Space Flight Center, Huntsville, AL 35812	
(Attn: S&E-ASTN-ES/Mr. E. E. Engler)	1
(Attn: S&E-ASTN-M/Mr. R. Schwinghamer)	1
(Attn: S&E-ASTM-MNM/Dr. J. M. Stuckey)	1
NASA, Langley Research Center, Hampton, VA 23365	3
(Attn: Mr. J. P. Peterson, Mr. R. Pride, and Dr. M. Card). .	
NASA, Lewis Research Center, Cleveland, OH 44153	2
(Attn: Technical Library, and M. Hershberg).	
NAVPGSCHL, Monterey, CA 95940	2
(Attn: Prof. R. Ball, Prof. M. H. Bank).	
NAVSEASYSCOM, Washington, D.C. 20362	1
(Attn: Code 035, Mr. C. Pohler).	
NAVSEC, Hyattsville, MD 20782	1
(Attn: Code 6101E03, Mr. W. Graner).	
NAVSHIPRANDCEN, Bethesda, MD 20034	1
(Attn: Code 173.2, Mr. W. P. Cauch).	
NAVSHIPRANDCEN, Annapolis, MD 21402	1
(Attn: Code 2870, Mr. H. Edelstein).	
NOL, White Oak, MD 20910	1
(Attn: Mr. F. R. Barnet).	
NRL, Washington, D.C. 20375	1
(Attn: Dr. I. Wolock).	
ONR, Washington, D.C. 20362	1
(Attn: Dr. N. Perrone)	

Government Activities (Cont.)

PLASTEC, Picatinny Arsenal, Dover, NJ 07801
(Attn: Librarian, Bldg. 176, SARPA-FR-M-D and Mr. H. Pebly). . 2
Scientific & Technical Information Facility, College Park, MD
(Attn: NASA Representative). 1
USAAVMATLAB, Fort Eustis, VA 23603
(Attn: Mr. R. Beresford) 1
USAMATRESAG, Watertown, MA
(Attn: Dr. E. Lenoe) 1
USARESOFC, Durham, NC 27701 1

Non-Government Agencies

Avco Aero Structures Division, Nashville, TN 37202
(Attn: Mr. W. Ottenville). 1
Battelle Columbus Laboratories, Metals and Ceramics Information
Center, 505 King Avenue, OH 43201. 1
Bell Aerospace Company, Buffalo, NY 14240
(Attn: Zone I-85, Mr. F. M. Anthony) 1
Bell Helicopter Company, Fort Worth, TX 76100
(Attn: Mr. Charles Harvey) 1
Bendix Products Aerospace Division, South Bend, IN 46619
(Attn: Mr. R. V. Cervelli) 1
Boeing Aerospace Company, P.O. Box 3999, Seattle, WA 98124
(Attn: Code 206, Mr. R. E. Horton) 1
Boeing Company, Renton, Washington 98055
(Attn: Dr. R. June). 1
Boeing Company, Vertol Division, Phila., PA 19142
(Attn: Mr. R. L. Pinckney, Mr. D. Hoffstedt) 2
Boeing Company, Wichita, KS 67210
(Attn: Mr. V. Reneau/MS 16-39) 1
Cabot Corporation, Billerica Research Center, Billerica, MA
01821 1
Drexel University, Phila., PA 19104
(Attn: Dr. P. C. Chou) 1
E.I. DuPont Company, Wilmington, DE 19898
(Attn: Dr. Carl Zweben) Bldg. 262/Room 316 1
Fairchild Industries, Hagerstown, MD 21740
(Attn: Mr. D. Ruck). 1
Georgia Institute of Technology, Atlanta, GA
(Attn: Prof. W. H. Horton) 1
General Dynamics/Convair, San Diego, CA 92138
(Attn: Mr. D. R. Dunbar, W. G. Scheck) 2
General Dynamics, Fort Worth, TX 76101
(Attn: Mr. P. D. Shockey, Dept. 23, Mail Zone P-46). 1
General Electric Company, Phila., PA 19101
(Attn: Mr. L. McCreight) 1
Great Lakes Carbon Corp., N.Y., NY 10017
(Attn: Mr. W. R. Benn, Mgr., Markey Development) 1
Grumman Aerospace Corporation, Bethpage, L.I., NY 11714
(Attn: Mr. R. Hadcock, Mr. S. Dastin). 2

2

Non-Government Agencies (Cont.)

Hercules Powder Company, Inc., Cumberland, MD 21501
(Attn: Mr. D. Hug) 1
H. I. Thompson Fiber Glass Company, Gardena, CA 90249
(Attn: Mr. N. Myers) 1
ITT Research Institute, Chicago, IL 60616
(Attn: Mr. K. Hofar) 1
J. P. Stevens & Co., Inc., N.Y., NY 10036
(Attn: Mr. H. I. Shulock). 1
Kaman Aircraft Corporation, Bloomfield, CT 06002
(Attn: Tech. Library). 1
Lehigh University, Bethlehem, PA 18015
(Attn: Dr. G. C. Sih). 1
Lockheed-California Company, Burbank, CA 91520
(Attn: Mr. E. K. Walker, R. L. Vaughn) 2
Lockheed-Georgia Company, Marietta, GA
(Attn: Advanced Composites Information Center, Dept. 72-14,
Zone 42). 1
LTV Aerospace Corporation, Dallas, TX 75222
(Attn: Mr. O. E. Dhonau/2-53442, C. R. Foreman). 2
Martin Company, Baltimore, MD 21203
(Attn: Mr. J. E. Pawken) 1
Materials Sciences Corp., Blue Bell, PA 19422 1
McDonnell Douglas Corporation, St. Louis, MO 63166
(Attn: Mr. R. C. Goran, O. B. McBee, C. Stenberg). 3
McDonnell Douglas Corporation, Long Beach, CA 90801
(Attn: H. C. Schjulderup, G. Lehman) 2
Minnesota Mining and Manufacturing Company, St. Paul, MN 55104
(Attn: Mr. W. Davis) 1
Northrop Aircraft Corp., Norair Div., Hawthorne, CA 90250
(Attn: Mr. R. D. Hayes, J. V. Noyes, R. C. Isemann). 3
Rockwell International, Columbus, OH 43216
(Attn: Mr. O. G. Acker, K. Clayton). 2
Rockwell International, Los Angeles, CA 90053
(Attn: Dr. L. Lackman) 1
Rockwell International, Tulsa, OK 74151
(Attn: Mr. E. Sanders, Mr. J. H. Powell) 2
Owens Corning Fiberglass, Granville, OH 43023
(Attn: Mr. D. Mettes). 1
Rohr Corporation, Riverside, CA 92503
(Attn: Dr. F. Riel and Mr. R. Elkin) 2
Ryan Aeronautical Company, San Diego, CA 92112
(Attn: Mr. R. Long). 1
Sikorsky Aircraft, Stratford, CT 06497
(Attn: Mr. J. Ray) 1
University of Oklahoma, Norman, OK 93069
(Attn: Dr. G. M. Nordby) 1
Union Carbide Corporation, Cleveland, OH 44101
(Attn: Dr. H. F. Volk) 1